MATHEMATICS OF COMPUTATION
Volume 00, Number 0, Pages 000–000
S 0025-5718(XX)0000-0

ANALYSIS OF THE BOUNDARY CONDITIONS FOR THE ULTRAWEAK-LOCAL DISCONTINUOUS GALERKIN METHOD OF TIME-DEPENDENT LINEAR FOURTH-ORDER PROBLEMS

FENGYU FU, CHI-WANG SHU, QI TAO, AND BOYING WU

Abstract. In this paper, we study the ultraweak-local discontinuous Galerkin (UWLDG) method for time-dependent linear fourth-order problems with four types of boundary conditions. In one dimension and two dimensions, stability and optimal error estimates of order $k+1$ are derived for the UWLDG scheme with polynomials of degree at most k ($k \geq 1$) for solving initial-boundary value problems. The main difficulties are the design of suitable penalty terms at the boundary for numerical fluxes and the construction of projections. More precisely, in two dimensions with the Dirichlet boundary condition, an elaborate projection of the exact boundary condition is proposed as the boundary flux, which, in combination with some proper penalty terms, leads to the stability and optimal error estimates. For other three types of boundary conditions, optimal error estimates can also be proved for fluxes without any penalty terms when special projections are designed to match different boundary conditions. Numerical experiments are presented to confirm the sharpness of theoretical results.

1. Introduction

In [29], Tao, Xu and Shu developed the ultraweak-local discontinuous Galerkin (UWLDG) method for partial differential equations (PDEs) involving high order spatial derivatives with periodic boundary conditions, in which stability and optimal error estimates are shown. In this paper, we are interested in analyzing the UWLDG method for initial-boundary value problems of the following time-dependent linear fourth-order equation

$$u_t + \Delta^2 u = 0, \quad (\boldsymbol{x}, t) \in \Omega \times (0, T], \quad u(\boldsymbol{x}, 0) = u_0(\boldsymbol{x}), \quad \boldsymbol{x} \in \Omega, \tag{1.1}$$

equipped with one of the four types of boundary conditions specified below.

(I) The Dirichlet boundary condition (Dirichlet B.C.)

$$u = f_D, \qquad \frac{\partial u}{\partial \boldsymbol{\nu}} = f_N, \quad \text{on } \partial\Omega; \tag{1.2a}$$

(II) The generalized Dirichlet boundary condition (G-Dirichlet B.C.)

$$u = f_D, \qquad \Delta u = g_D, \quad \text{on } \partial\Omega; \tag{1.2b}$$

1991 *Mathematics Subject Classification.* Primary 65M12, 65M15, 65M60.

Key words and phrases. fourth-order problem, UWLDG method, boundary conditions, optimal error estimates.

The research of the second author was supported by NSF grant DMS-2309249.

The research of the third author was supported by NSFC grant 12301464.

The research of the fourth author was supported by NSFC grant 12371419.

(III) The Neumann boundary condition (Neumann B.C.)

$$\frac{\partial u}{\partial \boldsymbol{\nu}} = f_N, \qquad \frac{\partial \Delta u}{\partial \boldsymbol{\nu}} = g_N, \quad \text{on } \partial\Omega; \tag{1.2c}$$

(IV) The mixed boundary condition (mixed B.C.)

$$\begin{aligned} u &= f_D, \qquad \Delta u = g_D, \qquad \text{on } \Gamma_D, \\ \frac{\partial u}{\partial \boldsymbol{\nu}} &= f_N, \qquad \frac{\partial \Delta u}{\partial \boldsymbol{\nu}} = g_N, \quad \text{on } \Gamma_N, \end{aligned} \tag{1.2d}$$

where $\Omega \subset \mathbb{R}^d$ $(d \geq 1)$ is a bounded Cartesian domain with boundary $\partial\Omega$, $\boldsymbol{\nu}$ is the unit outward normal direction to the boundary $\partial\Omega$, Γ_D and Γ_N are the parts of $\partial\Omega$ such that $\Gamma_D \cup \Gamma_N = \partial\Omega$, $\Gamma_D \cap \Gamma_N = \emptyset$. We assume $u_0(\boldsymbol{x})$, f_D, g_D, f_N, g_N are sufficiently smooth functions that make the problem (1.1) have a unique exact solution. The fourth-order boundary-value problems associated with (1.2a)–(1.2d) appear in many physical and engineering fields, such as strain gradient elasticity, deformation of beams modeling, plates deflection theory, phase separation in binary mixtures and image processing; see e.g., [2, 4, 16]. In particular, the Neumann B.C. (1.2c) is also called Cahn–Hilliard (C-H) type in the literature [3, 5], which is related to the C–H model of the phase-separation phenomena.

As a class of nonconforming finite element methods, the discontinuous Galerkin (DG) method was mainly designed for solving hyperbolic conservation laws; see, e.g., [13, 26]. To solve equations containing high order derivatives including fourth-order PDEs, different variants of DG methods are proposed. Let us first mention some work for steady-state fourth-order boundary-value problems. As the pioneering work [1], Baker applied the DG method to the approximation of the biharmonic equation with homogeneous Dirichlet B.C.. Subsequently, other types of DG methods are developed for fourth-order elliptic boundary-value problems, including the popular C^0 interior penalty DG (IPDG) method [3, 16], *hp*-version symmetric, nonsymmetric and semi-symmetric IPDG methods [15, 18, 25, 27], mixed DG (MDG) methods [19] and single face-hybridizable DG method [11], just to mention a few. For time-dependent fourth-order problems, there are relatively fewer results than that of the steady-state case, especially for non-homogeneous boundary-value problems. For example, several DG methods have been proposed for C-H equations [17, 23, 31]. An adaptive IPDG method was presented for a fully discrete approximation of the problem (1.1) with homogeneous Dirichlet B.C. [18]. In 2009, Dong and Shu [14] applied the local discontinuous Galerkin (LDG) method to the equation (1.1) with periodic boundary conditions, and derived optimal error estimates for Cartesian and triangular meshes. In [24, Example 3.3], a minimal-dissipation LDG scheme with some suitable boundary penalty terms was numerically investigated for the one-dimensional version of (1.1) with the Dirichlet B.C., and the optimal convergence rate was observed. In [21], an MDG scheme without interior penalty terms was proposed for (1.1) with boundary conditions (1.2a)–(1.2c), in which the stability was shown and analysis for the optimal error estimates was left to future work.

The UWLDG method was proposed and investigated in [7, 22, 28, 29, 30], its main feature is the combination of the advantages of LDG [12] and UWDG [8] methodologies. Taking the time-dependent linear fourth-order equation as an example, the UWLDG method rewrites the original equation into a second order

system by introducing the auxiliary variable $w = \Delta u$ and then performs integration by parts twice to each second order equation. This method is beneficial for solving higher order PDEs, since interior penalty terms are no long needed to ensure stability and fewer auxiliary variables are introduced, resulting in a more compact and efficient scheme.

To our best knowledge, existing theoretical results in the DG framework for time-dependent fourth-order problems are mainly focused on periodic boundary conditions, and discussions of general boundary conditions are very few. The main technicality may lie in the suitable design of numerical boundary conditions. From the perspective of theoretical analysis, the special choice of numerical initial condition is subtle for many high order PDEs [20, 32]. Analogously, in this paper, we find that, an appropriate choice of numerical boundary condition is also essential to ensure optimal error estimates for fourth-order PDEs with different types of boundary conditions. From the perspective of numerical experiments, for initial discretization, we know that a special choice of numerical initial condition is not always necessary; see, e.g., [20, Example 5.2] and [32, Remark 2.2]. However, in the numerical experiments of our current work, we would like to emphasize that the numerical boundary condition should be chosen as the same as that in theoretical analysis; otherwise, optimal order of accuracy cannot be observed. This may indicate that the numerical boundary condition seems to be more sensitive than the numerical initial condition, as far as the time-dependent linear fourth-order problems are considered.

The purpose of this paper is to construct the UWLDG scheme with delicate numerical boundary conditions and derive optimal error estimates for the equation (1.1) with four types of non-homogeneous boundary conditions in one dimension and two dimensions. Inspired by the minimal dissipation idea [6, 10], this work is devoted to design a DG scheme with optimal convergence rates using as few penalty terms as possible to treat different kinds of boundary conditions. The main difficulties are two folds. The first one is the proper choice of numerical fluxes for interior faces and the design of suitable penalty terms for boundary faces, especially when the Dirichlet B.C. is concerned; for other three types of boundary conditions, we present optimal convergent schemes without any penalty terms by carefully choosing the alternative interior fluxes to match the boundary conditions. Another difficulty is the construction and analysis of some elaborate projections, which help us to eliminate as many projection error terms as possible. In particular, in two dimensions, a superconvergent property of the projection in Lemmas 3.13–3.14 is essential for deriving optimal error estimates, which is achieved by establishing the almost polynomials preserving property of degree up to $k+2$ in Lemmas 3.11–3.12.

This paper is organized as follows. In Section 2, we present the UWLDG scheme and show the stability as well as optimal error estimates for the one-dimensional fourth-order problem (1.1) with four types of boundary conditions in (1.2a)–(1.2d). In Section 3, we extend the results to the two-dimensional case, in which numerical boundary conditions and projections are carefully investigated. In Section 4, we provide numerical experiments to confirm the theoretical results. We end in Section 5 with some concluding remarks.

Throughout the paper, we use the standard notation for Sobolev spaces and norms, i.e., $W^{m,p}(D)$ for $D \subseteq \Omega$ equipped with the norm $\|\cdot\|_{m,p,D}$; when $p = 2$, set $W^{m,2}(D) = H^m(D)$, $\|\cdot\|_{m,2,D} = \|\cdot\|_{m,D}$. For any partition Ω_h of the domain

Ω, the broken Sobolev space $H^\ell(\Omega_h)$ with ℓ being a positive integer is the space of functions that are piecewise in H^ℓ Sobolev space , and the associated norms can be piecewise defined. We denote $\|\cdot\|_{\ell,2,\Omega_h}$ by $\|\cdot\|_\ell$ when there is no confusion. We use $\|\cdot\|_D$ to denote the L^2 norm in D, and we omit the index D if $D=\Omega$ or Ω_h.

2. The UWLDG method for the 1D case

In this section, to clearly display the main idea of the numerical treatment of various boundary conditions, we consider the following one-dimensional version of time-dependent linear fourth-order equation (1.1) in the form:

$$u_t + u_{xxxx} = 0, \quad (x,t)\in\Omega\times(0,T], \quad u(x,0)=u_0(x), \tag{2.1}$$

with $\Omega=[a,b]$ and boundary conditions

$$\text{(i)}\ \ u(a,t)=f_0(t),\ u(b,t)=g_0(t),\ u_x(a,t)=f_1(t),\ u_x(b,t)=g_1(t), \tag{2.2a}$$
$$\text{(ii)}\ \ u(a,t)=f_0(t),\ u(b,t)=g_0(t),\ u_{xx}(a,t)=f_2(t),\ u_{xx}(b,t)=g_2(t), \tag{2.2b}$$
$$\text{(iii)}\ \ u_x(a,t)=f_1(t),\ u_x(b,t)=g_1(t),\ u_{xxx}(a,t)=f_3(t),\ u_{xxx}(b,t)=g_3(t), \tag{2.2c}$$
$$\text{(iv)}\ \ u(b,t)=g_0(t),\ u_x(a,t)=f_1(t),\ u_{xx}(b,t)=g_2(t),\ u_{xxx}(a,t)=f_3(t), \tag{2.2d}$$

where $u_0(x)$, $f_i(t), g_i(t)$, $i=0,1,2,3$ are sufficiently smooth functions.

2.1. The UWLDG scheme.

As usual, we divide the computational domain $\Omega=[a,b]$ into N cells

$$a = x_{\frac12} < x_{\frac32} < \cdots < x_{N+\frac12} = b,$$

and denote

$$I_j = \left(x_{j-\frac12},\ x_{j+\frac12}\right), \quad h_j = x_{j+\frac12}-x_{j-\frac12}, \quad \Omega_h=\{I_j\},$$

as the cells, cell lengths and the partition of Ω, respectively. We also define $h=\max_j h_j$ and assume the mesh is regular. We take the following piecewise polynomial finite element space

$$V_h = \{v : v|_{I_j}\in\mathcal{P}^k(I_j),\ j\in Z_N\}, \quad Z_N=\{1,\dots,N\},$$

where $\mathcal{P}^k(I_j)$ denotes the space of polynomials in I_j of degree at most k . We use $(v_h)^-_{j+\frac12}$ and $(v_h)^+_{j+\frac12}$ to denote the value of v_h at $x_{j+\frac12}$ from the left and right cells, respectively. Furthermore, the jump of v_h at $x_{j+\frac12}$ is defined as

$$[\![v_h]\!]_{j+\frac12} = (v_h)^+_{j+\frac12} - (v_h)^-_{j+\frac12}.$$

In order to construct the UWLDG scheme, we firstly introduce an auxiliary variable w as the second order derivative of the exact solution u and rewrite the equation (2.1) into a second order system

$$u_t + w_{xx} = 0,$$
$$w - u_{xx} = 0.$$

Then, the UWLDG scheme is defined as follows: find $u_h, w_h\in V_h$, such that for any $p,q\in V_h$ and $j\in Z_N$

$$((u_h)_t,p)_j + (w_h,p_{xx})_j + \widehat{w_x}p^-|_{j+\frac12} - \widehat{w_x}p^+|_{j-\frac12} - \widehat{w}p_x^-|_{j+\frac12} + \widehat{w}p_x^+|_{j-\frac12} = 0, \tag{2.3a}$$
$$(w_h,q)_j - (u_h,q_{xx})_j - \widehat{u_x}q^-|_{j+\frac12} + \widehat{u_x}q^+|_{j-\frac12} + \widehat{u}q_x^-|_{j+\frac12} - \widehat{u}q_x^+|_{j-\frac12} = 0. \tag{2.3b}$$

Here, $(u,v)_j = \int_{I_j} uv\,dx$, and $\widehat{u}$, $\widehat{u_x}$, $\widehat{w}$, $\widehat{w_x}$ are numerical fluxes, which will be specified later tailored to different type of boundary conditions.

To finish the construction of the UWLDG scheme, we now define the numerical flux according to the prescribed boundary conditions in (2.2a)–(2.2d). At interior points $x_{j+\frac{1}{2}}$, $j=1,\dots,N-1$, we choose

$$(\widehat{u},\ \widehat{u_x},\ \widehat{w},\ \widehat{w_x})_{j+\frac{1}{2}} = \big(u_h^+,\ (u_h)_x^-,\ w_h^+,\ (w_h)_x^-\big)_{j+\frac{1}{2}}, \tag{2.4}$$

for all four kinds of boundary conditions in (2.2a)–(2.2d); at boundary points $x_{\frac{1}{2}}$, $x_{N+\frac{1}{2}}$, we define:

Case (i) For the Dirichlet B.C. (2.2a),

$$(\widehat{u},\widehat{u_x},\widehat{w},\widehat{w_x})_{\frac{1}{2}} = \big(f_0(t),\ f_1(t),\ w_h^+,\ (w_h)_x^+ - \frac{k_2}{h^3}[\![u_h]\!]\big)_{\frac{1}{2}}, \tag{2.5a}$$

$$(\widehat{u},\widehat{u_x},\widehat{w},\widehat{w_x})_{N+\frac{1}{2}} = \big(g_0(t),\ g_1(t),\ w_h^- + \frac{k_1}{h}[\![(u_h)_x]\!],\ (w_h)_x^-\big)_{N+\frac{1}{2}}, \tag{2.5b}$$

where k_1, k_2 are positive constants independent of h and the polynomial degree k. Here and below, we set

$$(u_h)^-_{\frac{1}{2}} := f_0(t), \quad (u_h)^+_{N+\frac{1}{2}} := g_0(t), \quad \big((u_h)_x\big)^-_{\frac{1}{2}} := f_1(t), \quad \big((u_h)_x\big)^+_{N+\frac{1}{2}} := g_1(t),$$

to make the penalty terms well-defined.

Case (ii) For the G-Dirichlet B.C. (2.2b),

$$(\widehat{u},\widehat{u_x},\widehat{w},\widehat{w_x})_{\frac{1}{2}} = \big(f_0(t),\ (u_h)_x^+,\ f_2(t),\ (w_h)_x^+\big)_{\frac{1}{2}}, \tag{2.6a}$$

$$(\widehat{u},\widehat{u_x},\widehat{w},\widehat{w_x})_{N+\frac{1}{2}} = \big(g_0(t),\ (u_h)_x^-,\ g_2(t),\ (w_h)_x^-\big)_{N+\frac{1}{2}}. \tag{2.6b}$$

Case (iii) For the Neumann B.C. (2.2c),

$$(\widehat{u},\widehat{u_x},\widehat{w},\widehat{w_x})_{\frac{1}{2}} = \big(u_h^+,\ f_1(t),\ w_h^+,\ f_3(t)\big)_{\frac{1}{2}}, \tag{2.7a}$$

$$(\widehat{u},\widehat{u_x},\widehat{w},\widehat{w_x})_{N+\frac{1}{2}} = \big(u_h^-,\ g_1(t),\ w_h^-,\ g_3(t)\big)_{N+\frac{1}{2}}. \tag{2.7b}$$

Case (iv) For the mixed B.C. (2.2d),

$$(\widehat{u},\widehat{u_x},\widehat{w},\widehat{w_x})_{\frac{1}{2}} = \big(u_h^+,\ f_1(t),\ w_h^+,\ f_3(t)\big)_{\frac{1}{2}}, \tag{2.8a}$$

$$(\widehat{u},\widehat{u_x},\widehat{w},\widehat{w_x})_{N+\frac{1}{2}} = \big(g_0(t),\ (u_h)_x^-,\ g_2(t),\ (w_h)_x^-\big)_{N+\frac{1}{2}}. \tag{2.8b}$$

Remark 2.1. It is worth pointing out that the choice of numerical flux is not unique for each kind of boundary condition, and some other numerical fluxes would also work as discussed below.

For the Dirichlet B.C. (2.2a), we can also choose the following three kinds of numerical fluxes (with k_1, k_2 being positive constants):

- $$(\widehat{u},\widehat{u_x},\widehat{w},\widehat{w_x})_{j+\frac{1}{2}} = \begin{cases} \big(f_0(t),\ f_1(t),\ w_h^+ + \frac{k_1}{h}[\![(u_h)_x]\!],\ (w_h)_x^+ - \frac{k_2}{h^3}[\![u_h]\!]\big)_{\frac{1}{2}}, & j=0,\\ \big(u_h^+,\ (u_h)_x^+,\ w_h^-,\ (w_h)_x^-\big)_{j+\frac{1}{2}}, & j=1,\dots,N-1,\\ \big(g_0(t),\ g_1(t),\ w_h^-,\ (w_h)_x^-\big)_{N+\frac{1}{2}}, & j=N. \end{cases}$$

- $$(\widehat{u},\widehat{u_x},\widehat{w},\widehat{w_x})_{j+\frac{1}{2}} = \begin{cases} \big(f_0(t),\ f_1(t),\ w_h^+ + \frac{k_1}{h}[\![(u_h)_x]\!],\ (w_h)_x^+\big)_{\frac{1}{2}}, & j=0,\\ \big(u_h^-,\ (u_h)_x^+,\ w_h^-,\ (w_h)_x^+\big)_{j+\frac{1}{2}}, & j=1,\dots,N-1,\\ \big(g_0(t),\ g_1(t),\ w_h^-,\ (w_h)_x^- - \frac{k_2}{h^3}[\![u_h]\!]\big)_{N+\frac{1}{2}}, & j=N. \end{cases}$$

$$\bullet\ (\widehat{u},\ \widehat{u_x},\ \widehat{w},\ \widehat{w_x})_{j+\frac{1}{2}} = \begin{cases} \big(f_0(t),\ f_1(t),\ w_h^+,\ (w_h)_x^+\big)_{\frac{1}{2}},\ j=0, \\ \big(u_h^-,\ (u_h)_x^-,\ w_h^+,\ (w_h)_x^+\big)_{j+\frac{1}{2}},\ j=1,\dots,N-1, \\ \big(g_0(t),\ g_1(t), w_h^- + \frac{k_1}{h}\left[\!\left[(u_h)_x\right]\!\right], (w_h)_x^- - \frac{k_2}{h^3}\left[\!\left[u_h\right]\!\right]\big)_{N+\frac{1}{2}},\ j=N. \end{cases}$$

For the G-Dirichlet B.C. (2.2b), the Neumann B.C. (2.2c) and the mixed B.C. (2.2d), we can also choose the following numerical flux at interior points $x_{j+\frac{1}{2}}$, $j=1,\dots,N-1$, coupled with the boundary fluxes (2.6)–(2.8), respectively.

$$(\widehat{u},\ \widehat{u_x},\ \widehat{w},\ \widehat{w_x})_{j+\frac{1}{2}} = \big(u_h^-,\ (u_h)_x^+,\ w_h^-,\ (w_h)_x^+\big)_{j+\frac{1}{2}},\quad j=1,\dots,N-1. \tag{2.9}$$

Remark 2.2. In particular, if the equation (2.1) is equipped with the following type of mixed B.C.

$$u(a,t)=f_0(t),\ u_x(b,t)=g_1(t),\ u_{xx}(a,t)=f_2(t),\ u_{xxx}(b,t)=g_3(t),$$

we can take the numerical flux at interior points as (2.4) or (2.9), coupled with the following boundary flux:

$$(\widehat{u},\ \widehat{u_x},\ \widehat{w},\ \widehat{w_x})_{\frac{1}{2}} = \big(f_0(t),\ (u_h)_x^+,\ f_2(t),\ (w_h)_x^+\big)_{\frac{1}{2}},$$
$$(\widehat{u},\ \widehat{u_x},\ \widehat{w},\ \widehat{w_x})_{N+\frac{1}{2}} = \big(u_h^-,\ g_1(t),\ w_h^-,\ g_3(t)\big)_{N+\frac{1}{2}}.$$

In the following analysis, without loss of generality, we mainly consider the interior numerical flux (2.4) and the boundary fluxes (2.5)–(2.8) corresponding to boundary conditions (2.2a)–(2.2d), respectively.

2.2. **Stability analysis.** In this subsection, we will show the stability property of the scheme (2.3) with the interior numerical flux (2.4) and the boundary numerical fluxes in (2.5)–(2.8).

Theorem 2.3. *For the fourth-order problem* (2.1) *with the homogeneous boundary conditions in* (2.2a)–(2.2d)*, the solutions* u_h*,* w_h *to the semi-discrete UWLDG scheme* (2.3) *with numerical fluxes* (2.4) *and* (2.5)–(2.8) *satisfy the following* L^2 *stability*

$$\frac{1}{2}\frac{d}{dt}\|u_h(t)\|^2 + \|w_h(t)\|^2 \le 0. \tag{2.11}$$

Proof. We take the test function $p=u_h$, $q=w_h$ in (2.3), then use integration by parts and add the two equations together to obtain

$$((u_h)_t, u_h)_j + (w_h, w_h)_j + L_j^1(w_h,u_h) - L_j^2(u_h,w_h) = 0,\ \forall j \in Z_N, \tag{2.12}$$

where

$$\begin{aligned} L_j^1(w_h,u_h) =& w_h^-(u_h)_x^-|_{j+\frac{1}{2}} - w_h^+(u_h)_x^+|_{j-\frac{1}{2}} + \widehat{w_x}\,u_h^-|_{j+\frac{1}{2}} - \widehat{w_x}\,u_h^+|_{j-\frac{1}{2}} \\ & - \widehat{w}\,(u_h)_x^-|_{j+\frac{1}{2}} + \widehat{w}\,(u_h)_x^+|_{j-\frac{1}{2}}, \end{aligned}$$

$$\begin{aligned} L_j^2(u_h,w_h) =& u_h^-(w_h)_x^-|_{j+\frac{1}{2}} - u_h^+(w_h)_x^+|_{j-\frac{1}{2}} + \widehat{u_x}\,w_h^-|_{j+\frac{1}{2}} - \widehat{u_x}\,w_h^+|_{j-\frac{1}{2}} \\ & - \widehat{u}\,(w_h)_x^-|_{j+\frac{1}{2}} + \widehat{u}\,(w_h)_x^+|_{j-\frac{1}{2}}. \end{aligned}$$

Then, summing over j for (2.12), we get

$$\frac{1}{2}\frac{d}{dt}\|u_h(t)\|^2 + \|w_h(t)\|^2 + L(u_h,w_h) = 0, \tag{2.13}$$

where

$$L(u_h, w_h) = \sum_{j=1}^{N} \big(L_j^1(w_h, u_h) - L_j^2(u_h, w_h)\big).$$

To estimate $L(u_h, w_h)$, we firstly substitute the interior numerical flux (2.4) into it to obtain

$$L(u_h, w_h) = \mathcal{A}_0 + \mathcal{A}_\star, \tag{2.14}$$

where

$$\mathcal{A}_0 = w_h^-(u_h)_x^-|_{N+\frac{1}{2}} - w_h^+(u_h)_x^+|_{\frac{1}{2}} - u_h^-(w_h)_x^-|_{N+\frac{1}{2}} + u_h^+(w_h)_x^+|_{\frac{1}{2}}, \tag{2.15a}$$

$$\begin{aligned}\mathcal{A}_\star = {} & \widehat{w_x}u_h^-|_{N+\frac{1}{2}} - \widehat{w_x}u_h^+|_{\frac{1}{2}} - \widehat{w}(u_h)_x^-|_{N+\frac{1}{2}} + \widehat{w}(u_h)_x^+|_{\frac{1}{2}} \\ & - \widehat{u_x}w_h^-|_{N+\frac{1}{2}} + \widehat{u_x}w_h^+|_{\frac{1}{2}} + \widehat{u}(w_h)_x^-|_{N+\frac{1}{2}} - \widehat{u}(w_h)_x^+|_{\frac{1}{2}}.\end{aligned} \tag{2.15b}$$

We then insert each of the boundary flux (2.5)–(2.8) into the expression of $\mathcal{A}_\star$ in (2.15b), and denote the corresponding result, respectively, as $\mathcal{A}_{(\mathrm{i})}, \mathcal{A}_{(\mathrm{ii})}, \mathcal{A}_{(\mathrm{iii})}, \mathcal{A}_{(\mathrm{iv})}$, to get

$$\begin{aligned}\mathcal{A}_{(\mathrm{i})} = {} & -\mathcal{A}_0 - f_0 \cdot (w_h)_x^+|_{\frac{1}{2}} + g_0 \cdot (w_h)_x^-|_{N+\frac{1}{2}} + f_1 w_h^+|_{\frac{1}{2}} - g_1 w_h^-|_{N+\frac{1}{2}} \\ & - \frac{k_1}{h}[\![(u_h)_x]\!](u_h)_x^-|_{N+\frac{1}{2}} + \frac{k_2}{h^3}[\![u_h]\!]u_h^+|_{\frac{1}{2}}, \\ \mathcal{A}_{(\mathrm{ii})} = {} & -\mathcal{A}_0 - f_0 \cdot (w_h)_x^+|_{\frac{1}{2}} + g_0 \cdot (w_h)_x^-|_{N+\frac{1}{2}} + f_2 \cdot (u_h)_x^+|_{\frac{1}{2}} - g_2 \cdot (u_h)_x^-|_{N+\frac{1}{2}}, \\ \mathcal{A}_{(\mathrm{iii})} = {} & -\mathcal{A}_0 + f_1 w_h^+|_{\frac{1}{2}} - g_1 w_h^-|_{N+\frac{1}{2}} - f_3 u_h^+|_{\frac{1}{2}} + g_3 u_h^-|_{N+\frac{1}{2}}, \\ \mathcal{A}_{(\mathrm{iv})} = {} & -\mathcal{A}_0 - f_0 \cdot (w_h)_x^+|_{\frac{1}{2}} + g_1 w_h^-|_{N+\frac{1}{2}} + f_2 \cdot (u_h)_x^+|_{\frac{1}{2}} + g_3 u_h^-|_{N+\frac{1}{2}}.\end{aligned}$$

Clearly, when $f_i = 0,\ g_i = 0,\ i = 0, 1, 2, 3$, we have

$$[\![u_h]\!]_{\frac{1}{2}} = (u_h)_{\frac{1}{2}}^+, \quad [\![(u_h)_x]\!]_{N+\frac{1}{2}} = -\big((u_h)_x\big)_{N+\frac{1}{2}}^-,$$

and

$$\begin{aligned}\mathcal{A}_{(\mathrm{i})} &= -\mathcal{A}_0 + \frac{k_1}{h}\left(\big((u_h)_x\big)_{N+\frac{1}{2}}^-\right)^2 + \frac{k_2}{h^3}\left((u_h)_{\frac{1}{2}}^+\right)^2, \\ \mathcal{A}_{(\mathrm{ii})} &= \mathcal{A}_{(\mathrm{iii})} = \mathcal{A}_{(\mathrm{iv})} = -\mathcal{A}_0.\end{aligned} \tag{2.16}$$

Since $k_1,\ k_2$ are positive constants, we find, by (2.14), that

$$L(u_h, w_h) \geq 0$$

holds for $\mathcal{A}_\star = \mathcal{A}_{(\mathrm{i})}, \mathcal{A}_{(\mathrm{ii})}, \mathcal{A}_{(\mathrm{iii})}, \mathcal{A}_{(\mathrm{iv})}$, corresponding to all four kinds of boundary conditions in (2.2a)–(2.2d). This, together with (2.13), implies the stability result (2.11). □

2.3. **Optimal error estimates.** In this subsection, we present the optimal error estimates of the UWLDG scheme. To do that, we introduce several projections that are needed in the error analysis.

2.3.1. *Projections.* Different projections are needed in dealing with different boundary conditions with the goal of eliminating as many projection errors as possible. Given $u \in H^2(\Omega_h)$, we define three kinds of one-dimensional projection onto V_h as follows.

- P_M: For $k \geq 1$, $j \in Z_N$, $\mathsf{P}_M|_{I_j} \in \mathcal{P}^k(I_j)$, such that, for $j = 1, \ldots, N$,

$$\int_{I_j} (u - \mathsf{P}_M u) v_h \, dx = 0, \quad \forall v_h \in \mathcal{P}^{k-2}(I_j), \tag{2.17a}$$

$$\mathsf{P}_M u\big(x^+_{j-\frac{1}{2}}\big) = u\big(x_{j-\frac{1}{2}}\big), \quad \big(\mathsf{P}_M u\big)_x\big(x^-_{j+\frac{1}{2}}\big) = u_x\big(x_{j+\frac{1}{2}}\big). \tag{2.17b}$$

- P_D: For $k \geq 1$, $j \in Z_N$, $\mathsf{P}_D|_{I_j} \in \mathcal{P}^k(I_j)$, such that, for $j = 1, \ldots, N-1$,

$$\int_{I_j} (u - \mathsf{P}_D u) v_h \, dx = 0, \quad \forall v_h \in \mathcal{P}^{k-2}(I_j), \tag{2.18a}$$

$$\mathsf{P}_D u\big(x^+_{j-\frac{1}{2}}\big) = u\big(x_{j-\frac{1}{2}}\big), \quad \big(\mathsf{P}_D u\big)_x\big(x^-_{j+\frac{1}{2}}\big) = u_x\big(x_{j+\frac{1}{2}}\big), \tag{2.18b}$$

and for $j = N$,

$$\int_{I_N} (u - \mathsf{P}_D u) v_h \, dx = 0, \quad \forall v_h \in \mathcal{P}^{k-2}(I_N), \tag{2.18c}$$

$$\mathsf{P}_D u\big(x^+_{N-\frac{1}{2}}\big) = u\big(x_{N-\frac{1}{2}}\big), \quad \mathsf{P}_D u\big(x^-_{N+\frac{1}{2}}\big) = u\big(x_{N+\frac{1}{2}}\big). \tag{2.18d}$$

- P_N: For $k \geq 2$, $j \in Z_N$, $\mathsf{P}_N|_{I_j} \in \mathcal{P}^k(I_j)$, such that, for $j = 2, \ldots, N$,

$$\int_{I_j} (u - \mathsf{P}_N u) v_h \, dx = 0, \quad \forall v_h \in \mathcal{P}^{k-2}(I_j), \tag{2.19a}$$

$$\mathsf{P}_N u\big(x^+_{j-\frac{1}{2}}\big) = u\big(x_{j-\frac{1}{2}}\big), \quad \big(\mathsf{P}_N u\big)_x\big(x^-_{j+\frac{1}{2}}\big) = u_x\big(x_{j+\frac{1}{2}}\big), \tag{2.19b}$$

and for $j = 1$,

$$\int_{I_1} (u - \mathsf{P}_N u) v_h \, dx = 0, \quad \forall v_h \in \mathcal{P}^{k-2}(I_1), \tag{2.19c}$$

$$(\mathsf{P}_N u)_x\big(x^+_{\frac{1}{2}}\big) = u_x\big(x_{\frac{1}{2}}\big), \quad (\mathsf{P}_N u)_x\big(x^-_{\frac{3}{2}}\big) = u_x\big(x_{\frac{3}{2}}\big). \tag{2.19d}$$

It is easy to verify that all these projections are well defined and have the following optimal approximation property; see [9, 29].

Lemma 2.4. *Let π be any projection defined by* (2.17)–(2.19)*, then for $u \in H^{k+1}(\Omega_h)$, there holds*

$$\|u - \pi u\| + h^s \|u - \pi u\|_s + h^{\frac{1}{2}} \|u - \pi u\|_{\Gamma_h} \leq C h^{k+1} \|u\|_{k+1}, \tag{2.20}$$

where $\|v\|_{\Gamma_h} = \Big(\sum_{j=1}^N \big[(v^-_{j+\frac{1}{2}})^2 + (v^+_{j-\frac{1}{2}})^2 \big] \Big)^{\frac{1}{2}}$, $1 \leq s \leq k$ is an integer and C is a positive constant independent of h.

2.3.2. *Main results.* Without loss of generality, we firstly state the error estimate result for the case of the Dirichlet B.C. (2.2a), and the results for other three boundary conditions will be discussed in Remark 2.6 and Remark 2.7.

Theorem 2.5. *Let u be the exact solution of the fourth-order equation* (2.1) *with the boundary condition* (2.2a)*, $w = u_{xx}$; and assume u is smooth enough, e.g., $\|u\|_{k+3}, \|u_t\|_{k+1}$ are bounded uniformly for any time t. Let u_h, w_h be solutions of*

the UWLDG scheme (2.3) *with numerical fluxes* (2.4)–(2.5). *Then, for* $k \geq 1$, *we have the following optimal error estimates:*

$$\|u(t) - u_h(t)\| + \int_0^t \|w(\tau) - w_h(\tau)\|\, d\tau \leq Ch^{k+1}, \tag{2.21}$$

where C *is a function of* t *to the power at most* $\frac{3}{2}$, *which is independent of* h, *and dependent on* $\|u\|_{k+3}$, $\|u_t\|_{k+1}$.

Proof. Let $e_u = u - u_h$, $e_w = w - w_h$. Since u and w also satisfy the UWLDG scheme (2.3)–(2.5), we sum over j for the cell error equations to get

$$\big((e_u)_t, p\big)_{\Omega_h} + B(e_w, p) = 0, \tag{2.22a}$$

$$(e_w, q)_{\Omega_h} - B(e_u, q) = 0, \tag{2.22b}$$

where $(\cdot,\cdot)_{\Omega_h}$ denotes the summation of the L^2 inner product in $I_j \in \Omega_h$, and $B(\cdot,\cdot)$ is defined as follows: for $v, z \in H^2(\Omega_h)$

$$B(v,z) = \sum_{j=1}^{N} (v, z_{xx})_j + \sum_{j=1}^{N} \Big(\widehat{v_x}\, z^-|_{j+\frac{1}{2}} - \widehat{v_x}\, z^+|_{j-\frac{1}{2}} - \widehat{v}\, z_x^-|_{j+\frac{1}{2}} + \widehat{v}\, z_x^+|_{j-\frac{1}{2}} \Big),$$

and

$$\Big(\widehat{e_u},\, \widehat{(e_u)_x},\, \widehat{e_w},\, \widehat{(e_w)_x}\Big)_{j+\frac{1}{2}} = \begin{cases} \big(0,\, 0,\, e_w^+,\, (e_w)_x^+ + \frac{k_2}{h^3}[\![u_h]\!]\big)_{\frac{1}{2}}, & j = 0, \\ \big(e_u^+,\, (e_u)_x^-,\, e_w^+,\, (e_w)_x^-\big)_{j+\frac{1}{2}}, & j = 1, \ldots, N-1, \\ \big(0,\, 0,\, e_w^- - \frac{k_1}{h}[\![(u_h)_x]\!],\, (e_w)_x^-\big)_{N+\frac{1}{2}}, & j = N. \end{cases}$$

Notice that $[\![u_h]\!]_{\frac{1}{2}} = -(e_u)^+_{\frac{1}{2}}$ and $[\![(u_h)_x]\!]_{N+\frac{1}{2}} = ((e_u)_x)^-_{N+\frac{1}{2}}$, then

$$\widehat{(e_w)_x}\big|_{\frac{1}{2}} = \big((e_w)_x\big)^+_{\frac{1}{2}} - \frac{k_2}{h^3}(e_u)^+_{\frac{1}{2}}, \quad \widehat{e_w}\big|_{N+\frac{1}{2}} = \big(e_w\big)^-_{N+\frac{1}{2}} - \frac{k_1}{h}\big((e_u)_x\big)^-_{N+\frac{1}{2}}.$$

Next, we denote

$$\begin{aligned} e_u &= (u - \mathsf{P}_M u) - (u_h - \mathsf{P}_M u) := \eta_u - \xi_u, \\ e_w &= (w - \mathsf{P}_M w) - (w_h - \mathsf{P}_M w) := \eta_w - \xi_w, \end{aligned}$$

and let

$$\Big(\widehat{\eta_u},\, \widehat{(\eta_u)_x},\, \widehat{\eta_w},\, \widehat{(\eta_w)_x}\Big)_{j+\frac{1}{2}} = \begin{cases} \big(0,\, 0,\, \eta_w^+,\, (\eta_w)_x^+ - \frac{k_2}{h^3}\eta_u^+\big)_{\frac{1}{2}}, & j = 0, \\ \big(\eta_u^+,\, (\eta_u)_x^-,\, \eta_w^+,\, (\eta_w)_x^-\big)_{j+\frac{1}{2}}, & j = 1, \ldots, N-1, \\ \big(0,\, 0,\, \eta_w^- - \frac{k_1}{h}(\eta_u)_x^-,\, (\eta_w)_x^-\big)_{N+\frac{1}{2}}, & j = N, \end{cases}$$

$$\Big(\widehat{\xi_u},\, \widehat{(\xi_u)_x},\, \widehat{\xi_w},\, \widehat{(\xi_w)_x}\Big)_{j+\frac{1}{2}} = \begin{cases} \big(0,\, 0,\, \xi_w^+,\, (\xi_w)_x^+ - \frac{k_2}{h^3}\xi_u^+\big)_{\frac{1}{2}}, & j = 0, \\ \big(\xi_u^+,\, (\xi_u)_x^-,\, \xi_w^+,\, (\xi_w)_x^-\big)_{j+\frac{1}{2}}, & j = 1, \ldots, N-1, \\ \big(0,\, 0,\, \xi_w^- - \frac{k_1}{h}(\xi_u)_x^-,\, (\xi_w)_x^-\big)_{N+\frac{1}{2}}, & j = N. \end{cases}$$

Then, taking $p = \xi_u$, $q = \xi_w$ and adding the two equations in (2.22), we get

$$LHS = RHS,$$

where

$$\begin{aligned} LHS &= \big((\xi_u)_t, \xi_u\big)_{\Omega_h} + (\xi_w, \xi_w)_{\Omega_h} + B(\xi_w, \xi_u) - B(\xi_u, \xi_w), \\ RHS &= \big((\eta_u)_t, \xi_u\big)_{\Omega_h} + (\eta_w, \xi_w)_{\Omega_h} + B(\eta_w, \xi_u) - B(\eta_u, \xi_w). \end{aligned}$$

Using integration by parts and a simple calculation, we can get

$$LHS = \big((\xi_u)_t, \xi_u\big)_{\Omega_h} + (\xi_w, \xi_w)_{\Omega_h} + \frac{k_2}{h^3}\left((\xi_u)^+_{\frac{1}{2}}\right)^2 + \frac{k_1}{h}\left(\big((\xi_u)_x\big)^-_{N+\frac{1}{2}}\right)^2. \tag{2.23}$$

Besides, the definition of the projection P_M implies that

$$RHS = \big((\eta_u)_t, \xi_u\big)_{\Omega_h} + (\eta_w, \xi_w)_{\Omega_h} - \big((\eta_w)_x\big)^+_{\frac{1}{2}}(\xi_u)^+_{\frac{1}{2}} - (\eta_w)^-_{N+\frac{1}{2}}\big((\xi_u)_x\big)^-_{N+\frac{1}{2}}. \tag{2.24}$$

Using Young's inequality, we obtain

$$\begin{aligned} -\big((\eta_w)_x\big)^+_{\frac{1}{2}}(\xi_u)^+_{\frac{1}{2}} &\le \frac{h^3}{2k_2}\left(\big((\eta_w)_x\big)^+_{\frac{1}{2}}\right)^2 + \frac{k_2}{2h^3}\left((\xi_u)^+_{\frac{1}{2}}\right)^2, \\ -(\eta_w)^-_{N+\frac{1}{2}}\big((\xi_u)_x\big)^-_{N+\frac{1}{2}} &\le \frac{h}{2k_1}\left((\eta_w)^-_{N+\frac{1}{2}}\right)^2 + \frac{k_1}{2h}\left(\big((\xi_u)_x\big)^-_{N+\frac{1}{2}}\right)^2. \end{aligned} \tag{2.25}$$

Consequently, by the trace inequality and approximation property of the projection P_M in (2.20), we get

$$\big|\,((\eta_w)_x)^+_{\frac{1}{2}}\,\big| \le Ch^{k-\frac{1}{2}}\|w\|_{k+1}, \quad \big|(\eta_w)^-_{N+\frac{1}{2}}\big| \le Ch^{k+\frac{1}{2}}\|w\|_{k+1}. \tag{2.26}$$

Thus, it follows from Cauchy–Schwarz inequality and (2.23)–(2.26) that

$$\frac{1}{2}\frac{d}{dt}\|\xi_u(t)\|^2 + \|\xi_w(t)\|^2 \le Ch^{k+1}\|\xi_u(t)\| + Ch^{k+1}\|\xi_w(t)\| + Ch^{2k+2}. \tag{2.27}$$

Next, we adopt the idea in the proof of [21, Theorem 2.2] and omit the details to save space, and we arrive at

$$\|\xi_u(t)\| + \int_0^t \|\xi_w(\tau)\|\,d\tau \le Ch^{k+1},$$

where C is a function of t to the power at most $\frac{3}{2}$, which is dependent on $\|u\|_{k+3}$ and $\|u_t\|_{k+1}$, but is independent of h. Then, by the triangle inequality we finally get the error estimates result (2.21). □

Remark 2.6. For the fourth-order problem (2.1) with the G-Dirichlet B.C. (2.2b), the UWLDG solutions of (2.3) with numerical fluxes (2.4) and (2.6) satisfy the optimal error estimate result (2.21) for $k \ge 2$, which can be proved by performing the similar arguments as in the proof of Theorem 2.5 and using the projection P_N. For $k = 1$, we cannot prove the second order accuracy, indeed, only 3/2th order is observed in the numerical experiment for both L^2 error of u and w; see Table 4.2 and Table 4.3 in Section 4.

Remark 2.7. For the fourth-order problem (2.1) with the Neumann B.C. (2.2c) and the mixed B.C. (2.2d), consider the UWLDG solutions of (2.3) with interior flux (2.4) and the boundary fluxes (2.7)–(2.8), the optimal error estimates in (2.21) for $k \ge 1$ can also be proved by using the projections P_D and P_M, respectively.

3. The UWLDG method for the 2D case

In this section, we extend our methods to multi-dimensional case, and consider the Cartesian domain only. Without loss of generality, consider the UWLDG method for the two-dimensional time-dependent fourth-order problem (1.1) with boundary conditions (1.2a)–(1.2d). Let $\Omega = [a_1, b_1] \times [a_2, b_2]$ be a bounded rectangular domain, and denote

$$\Gamma_N = \{(x, y) \in \partial\Omega | x = a_1 \text{ or } y = a_2\}, \quad \Gamma_D = \{(x, y) \in \partial\Omega | x = b_1 \text{ or } y = b_2\}.$$

We set $\boldsymbol{\nu}_m$, $m = l, b, r, t$, are the unit outward normal vectors of the left, bottom, right and top boundary side of Ω respectively, i.e.,

$$\boldsymbol{\nu}_l = (-1, 0),\ \boldsymbol{\nu}_b = (0, -1),\ \boldsymbol{\nu}_r = (1, 0),\ \boldsymbol{\nu}_t = (0, 1).$$

3.1. **The UWLDG scheme.** Similar to the one-dimensional case, we rewrite (1.1) into a second order system

$$\begin{aligned} u_t + \Delta w &= 0, \\ w - \Delta u &= 0. \end{aligned}$$

To define the UWLDG method clearly, let us first introduce some notation.

3.1.1. *Notation.* As shown in Figure 3.1, let $\Omega_h = \{K_{ij} = I_i \times J_j,\ i = 1, \ldots, N_x,\ j = 1, \ldots, N_y\}$ be a partition of Ω with the shape-regular rectangle element K_{ij}. We denote Ω_h^I and Ω_h^0 as the sets of all the interelements and the boundary elements, respectively. We denote $\mathscr{E}_h$ as the set of all faces of the partition Ω_h, and $\mathscr{E}_h^I$, $\mathscr{E}_h^0$ as the sets of interior faces e (i.e., e is shared by two elements in Ω_h) and boundary faces e (i.e., e lies on $\partial\Omega$), respectively. In particular, $\mathscr{E}_h^{0,l}$, $\mathscr{E}_h^{0,b}$, $\mathscr{E}_h^{0,r}$ and $\mathscr{E}_h^{0,t}$ represent the sets of boundary faces e that lie on the left, bottom, right and top side of the domain Ω, respectively.

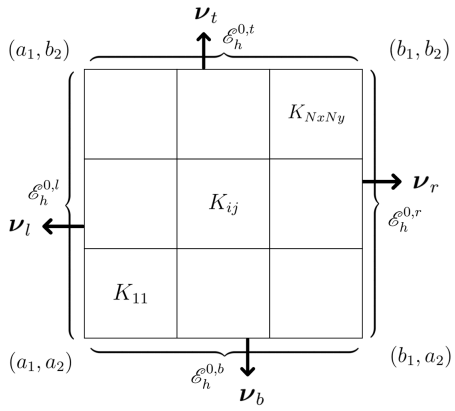

FIGURE 3.1. The 2D mesh Ω_h.

The boundary and the diameter of K are denoted as ∂K and h_K, and set $h = \max_K h_K$. The finite element space associated with the mesh Ω_h is of the form

$$W_h = \left\{ v \in L^2(\Omega) : v|_K \in \mathcal{Q}^k(K),\ \forall K \in \Omega_h \right\},$$

where $\mathcal{Q}^k(K)$ is the space of tensor product of polynomials of degree at most k in each variable of $\boldsymbol{x} = (x, y)$ in K.

3.1.2. *The UWLDG scheme.* The UWLDG method is given as follows: to seek $u_h, w_h \in W_h$, such that

$$\left((u_h)_t, p \right)_K + (w_h, \Delta p)_K + \langle \widehat{\nabla w} \cdot \mathbf{n}, p \rangle_{\partial K} - \langle \widehat{w}, \nabla p \cdot \mathbf{n} \rangle_{\partial K} = 0, \tag{3.2a}$$

$$(w_h, q)_K - (u_h, \Delta q)_K - \langle \widehat{\nabla u} \cdot \mathbf{n}, q \rangle_{\partial K} + \langle \widehat{u}, \nabla q \cdot \mathbf{n} \rangle_{\partial K} = 0, \tag{3.2b}$$

holds for all $p, q \in W_h$ and $K \in \Omega_h$. Here $\mathbf{n}$ denotes the unit outward normal vector to ∂K, and for any $v, z \in H^2(\Omega_h)$

$$(v,z)_K = \int_K v(x,y)z(x,y)\ dxdy, \quad \langle v, \nabla z \cdot \mathbf{n}\rangle_{\partial K} = \int_{\partial K} v(s)\big(\nabla z(s)\cdot \mathbf{n}\big)\ ds.$$

For the above boundary integral, if v or z is not single-valued on the element faces, we take its value from interior of K and restrict it on ∂K.

To complete the definition of the UWLDG method, we need to define the numerical fluxes $\widehat{u}$, $\widehat{\nabla u}$, $\widehat{w}$ and $\widehat{\nabla w}$. To do that, firstly, for a possibly discontinuous function $\omega(x,y)$, we define $\omega^{\pm}$ on the vertical and horizontal edge respectively as

$$\begin{aligned}
\omega^{\pm}_{i+\frac{1}{2},y} &= \omega\big(x^{\pm}_{i+\frac{1}{2}}, y\big) = \lim_{\varepsilon\to 0^{\pm}} \omega\big(x_{i+\frac{1}{2}}+\varepsilon,\ y\big), \quad i = 0,1,\ldots,N_x,\\
\omega^{\pm}_{x,j+\frac{1}{2}} &= \omega\big(x, y^{\pm}_{j+\frac{1}{2}}\big) = \lim_{\varepsilon\to 0^{\pm}} \omega\big(x,\ y_{j+\frac{1}{2}}+\varepsilon\big), \quad j = 0,1,\ldots,N_y.
\end{aligned}$$

We denote

$$\big(\nabla\omega\big)^{\pm}_{i+\frac{1}{2},y} = \big((\omega_x)^{\pm}_{i+\frac{1}{2},y},\ (\omega_y)^{\pm}_{i+\frac{1}{2},y}\big)^{\mathsf{T}}, \quad \big(\nabla\omega\big)^{\pm}_{x,j+\frac{1}{2}} = \big((\omega_x)^{\pm}_{x,j+\frac{1}{2}},\ (\omega_y)^{\pm}_{x,j+\frac{1}{2}}\big)^{\mathsf{T}},$$

and set the jump value as

$$[\![\omega]\!]_{i+\frac{1}{2},y} = \omega^{+}_{i+\frac{1}{2},y} - \omega^{-}_{i+\frac{1}{2},y}, \quad [\![\omega]\!]_{x,j+\frac{1}{2}} = \omega^{+}_{x,j+\frac{1}{2}} - \omega^{-}_{x,j+\frac{1}{2}}.$$

Then, the numerical fluxes are defined as follows. At interior faces $e \in \mathscr{E}_h^I$, we always choose

$$\widehat{u}\big|_e = u_h^+\big|_e,\ \widehat{\nabla u}\big|_e = (\nabla u_h)^-\big|_e,\ \widehat{w}\big|_e = w_h^+\big|_e,\ \widehat{\nabla w}\big|_e = (\nabla w_h)^-\big|_e. \tag{3.3}$$

For the numerical flux on the boundary face $e \in \mathscr{E}_h^0$, we firstly consider the Dirichlet B.C. (1.2a), since some penalty terms are involved.

Case (I) For the Dirichlet B.C. (1.2a), we define:

- the numerical flux $\widehat{u}\big|_e$ as

$$\widehat{u}\big|_e = \mathsf{P}_M\left(f_D\right)\big|_e, \quad \forall e \in \mathscr{E}_h^0; \tag{3.4a}$$

- the numerical flux $\widehat{\nabla u}\big|_e$ as

$$\widehat{\nabla u}\cdot\boldsymbol{\nu}_m\big|_e = \mathsf{P}_M\big(f_N\big)\big|_e, \quad \forall e \in \mathscr{E}_h^{0,m},\ m = l,b,r,t; \tag{3.4b}$$

- the numerical flux $\widehat{w}\big|_e$ as

$$\begin{aligned}
\widehat{w}\big|_e &= w_h^+\big|_e, && \forall e \in \mathscr{E}_h^{0,l}, \mathscr{E}_h^{0,b},\\
\widehat{w}\big|_e &= w_h^-\big|_e + \frac{k_1}{h}[\![(u_h)_x]\!]\big|_e, && \forall e \in \mathscr{E}_h^{0,r},\\
\widehat{w}\big|_e &= w_h^-\big|_e + \frac{k_2}{h}[\![(u_h)_y]\!]\big|_e, && \forall e \in \mathscr{E}_h^{0,t};
\end{aligned} \tag{3.4c}$$

- the numerical flux $\widehat{\nabla w}\big|_e$ as

$$\begin{aligned}
\widehat{\nabla w}\cdot\boldsymbol{\nu}_l\big|_e &= (\nabla w_h)^+\cdot\boldsymbol{\nu}_l\big|_e + \frac{k_3}{h^3}[\![u_h]\!]\big|_e, && \forall e \in \mathscr{E}_h^{0,l},\\
\widehat{\nabla w}\cdot\boldsymbol{\nu}_b\big|_e &= (\nabla w_h)^+\cdot\boldsymbol{\nu}_b\big|_e + \frac{k_4}{h^3}[\![u_h]\!]\big|_e, && \forall e \in \mathscr{E}_h^{0,b},\\
\widehat{\nabla w}\cdot\boldsymbol{\nu}_m\big|_e &= (\nabla w_h)^-\cdot\boldsymbol{\nu}_m\big|_e, && \forall e \in \mathscr{E}_h^{0,m}, m = r,\ t;
\end{aligned} \tag{3.4d}$$

where k_1, k_2, k_3, k_4 are positive constants independent of h and the polynomial degree k. To ensure the penalty terms in (3.4c) and (3.4d) are well-defined, we set

$$\begin{aligned} u_h^-\big|_e &:= \mathsf{P}_M(f_D)|_e, \ \forall e \in \mathscr{E}_h^{0,l}, \ \mathscr{E}_h^{0,b}, \\ \big((u_h)_x\big)^+\big|_e &:= \mathsf{P}_M\big(f_N\big)|_e, \ \forall e \in \mathscr{E}_h^{0,r}, \\ \big((u_h)_y\big)^+\big|_e &:= \mathsf{P}_M\big(f_N\big)|_e, \ \forall e \in \mathscr{E}_h^{0,t}. \end{aligned}$$

The numerical fluxes for other three types of boundary conditions are given in the following remark.

Remark 3.1. For boundary conditions (1.2b)–(1.2d), we can use the numerical flux (3.3) for interior face $e \in \mathscr{E}_h^I$ together with the following boundary flux for $e \in \mathscr{E}_h^0$.

Case (II) For the G-Dirichlet B.C. (1.2b), we define:

(3.5)
$$\begin{aligned} &\widehat{u}\big|_e = \mathsf{P}_N(f_D)\big|_e, \quad \widehat{w}\big|_e = \mathsf{P}_N(g_D)\big|_e, \quad \forall e \in \mathscr{E}_h^0, \\ &\widehat{\nabla u}\cdot\boldsymbol{\nu}_m\big|_e = (\nabla u_h)^+\cdot\boldsymbol{\nu}_m\big|_e, \ \widehat{\nabla w}\cdot\boldsymbol{\nu}_m\big|_e = (\nabla w_h)^+\cdot\boldsymbol{\nu}_m\big|_e, \ \forall e \in \mathscr{E}_h^{0,m}, m = l, b, \\ &\widehat{\nabla u}\cdot\boldsymbol{\nu}_m\big|_e = (\nabla u_h)^-\cdot\boldsymbol{\nu}_m\big|_e, \ \widehat{\nabla w}\cdot\boldsymbol{\nu}_m\big|_e = (\nabla w_h)^-\cdot\boldsymbol{\nu}_m\big|_e, \ \forall e \in \mathscr{E}_h^{0,m}, m = r, t. \end{aligned}$$

Case (III) For the Neumann B.C. (1.2c), we define:

(3.6)
$$\begin{aligned} &\widehat{u}\big|_e = u_h^+\big|_e, \quad \widehat{w}\big|_e = w_h^+\big|_e, \quad \forall e \in \mathscr{E}_h^{0,m}, m = l, b, \\ &\widehat{u}\big|_e = u_h^-\big|_e, \quad \widehat{w}\big|_e = w_h^-\big|_e, \quad \forall e \in \mathscr{E}_h^{0,m}, m = r, t, \\ &\widehat{\nabla u}\cdot\boldsymbol{\nu}_m\big|_e = \mathsf{P}_D(f_N)\big|_e, \quad \widehat{\nabla w}\cdot\boldsymbol{\nu}_m\big|_e = \mathsf{P}_D(g_N)\big|_e, \quad \forall e \in \mathscr{E}_h^{0,m}, m = l, b, r, t. \end{aligned}$$

Case (IV) For the mixed B.C. (1.2d), we define: for $e \in \mathscr{E}_h^{0,m}$, $m = l, b$,

(3.7a)
$$\widehat{u}\big|_e = u_h^+\big|_e, \ \widehat{\nabla u}\cdot\boldsymbol{\nu}_m\big|_e = \mathsf{P}_M(f_N)\big|_e, \ \widehat{w}\big|_e = w_h^+\big|_e, \ \widehat{\nabla w}\cdot\boldsymbol{\nu}_m\big|_e = \mathsf{P}_M(g_N)\big|_e,$$

and for $e \in \mathscr{E}_h^{0,m}$, $m = r, t$,

(3.7b)
$$\begin{aligned} &\widehat{u}\big|_e = \mathsf{P}_M(f_D)\big|_e, \quad \widehat{\nabla u}\cdot\boldsymbol{\nu}_m\big|_e = (\nabla u_h)^-\cdot\boldsymbol{\nu}_m\big|_e, \\ &\widehat{w}\big|_e = \mathsf{P}_M(g_D)\big|_e, \quad \widehat{\nabla w}\cdot\boldsymbol{\nu}_m\big|_e = (\nabla w_h)^-\cdot\boldsymbol{\nu}_m\big|_e. \end{aligned}$$

In the following subsections, we will give stability analysis and error estimate results of the above UWLDG schemes. Before that, for easy presentation, we introduce several short notations. Firstly, for $\eta \in H^2(\Omega_h)$ and $p \in W_h$, we define

$$B_K(\eta, p) = (\eta, \Delta p)_K + \langle\widehat{\nabla\eta}\cdot\mathbf{n}, p\rangle_{\partial K} - \langle\widehat{\eta}, \nabla p\cdot\mathbf{n}\rangle_{\partial K}, \ \forall\ K \in \Omega_h. \tag{3.8}$$

Then, for $K_{ij} \in \Omega_h^I$, we specifically have

$$B_{K_{ij}}(\eta, p) = \sum_{m=0}^{8} T_m^{ij}(\eta, p), \quad i = 2, 3, \ldots, N_x - 1, \ j = 2, 3, \ldots, N_y - 1, \tag{3.9}$$

where

(3.10)
$$\begin{aligned} &T_0^{ij}(\eta, p) = \int_{K_{ij}} \eta\,(p_{xx} + p_{yy})\,dxdy, \\ &T_1^{ij}(\eta, p) = -\int_{J_j} \eta(x_{i+\frac{1}{2}}^+, y)\,p_x(x_{i+\frac{1}{2}}^-, y)\,dy, \quad T_2^{ij}(\eta, p) = \int_{J_j} \eta(x_{i-\frac{1}{2}}^+, y)\,p_x(x_{i-\frac{1}{2}}^+, y)\,dy, \end{aligned}$$

$$T_3^{ij}(\eta,p)=-\int_{I_i}\eta(x,y^+_{j+\frac12})\,p_y(x,y^-_{j+\frac12})\,dx,\quad T_4^{ij}(\eta,p)=\int_{I_i}\eta(x,y^+_{j-\frac12})\,p_y(x,y^+_{j-\frac12})\,dx,$$
$$T_5^{ij}(\eta,p)=\int_{J_j}\eta_x(x^-_{i+\frac12},y)\,p(x^-_{i+\frac12},y)\,dy,\quad T_6^{ij}(\eta,p)=-\int_{J_j}\eta_x(x^-_{i-\frac12},y)\,p(x^+_{i-\frac12},y)\,dy,$$
$$T_7^{ij}(\eta,p)=\int_{I_i}\eta_y(x,y^-_{j+\frac12})\,p(x,y^-_{j+\frac12})\,dx,\quad T_8^{ij}(\eta,p)=-\int_{I_i}\eta_y(x,y^-_{j-\frac12})\,p(x,y^+_{j-\frac12})\,dx.$$

Next, for each $K\in\Omega_h$, $p,q,\varphi\in W_h$, we introduce

$$\begin{aligned}H_{\partial K}(p,q)=&\langle w_h,\nabla u_h\cdot\mathbf{n}\rangle_{\partial K}-\langle u_h,\nabla w_h\cdot\mathbf{n}\rangle_{\partial K}+\langle\widehat{\nabla w}\cdot\mathbf{n},p\rangle_{\partial K}\\&-\langle\widehat{w},\nabla p\cdot\mathbf{n}\rangle_{\partial K}-\langle\widehat{\nabla u}\cdot\mathbf{n},q\rangle_{\partial K}+\langle\widehat{u},\nabla q\cdot\mathbf{n}\rangle_{\partial K},\end{aligned}\tag{3.11}$$

and

$$\begin{aligned}S(\varphi)=&\sum_{j=1}^{N_y}\int_{J_j}\frac{k_1}{h}\left(\varphi_x(x^-_{N_x+\frac12},y)\right)^2+\frac{k_3}{h^3}\left(\varphi(x^+_{\frac12},y)\right)^2dy\\&+\sum_{i=1}^{N_x}\int_{I_i}\frac{k_2}{h}\left(\varphi_y(x,y^-_{N_y+\frac12})\right)^2+\frac{k_4}{h^3}\left(\varphi(x,y^+_{\frac12})\right)^2dx.\end{aligned}\tag{3.12}$$

3.2. **Stability analysis.** In this subsection, we show the L^2-stability of the UWLDG method (3.2) with the interior flux (3.3) and the boundary fluxes (3.4)–(3.7).

Lemma 3.2. *If the boundary condition* (1.2a) *is homogeneous, i.e.,* $f_D=0, f_N=0$*, on* $\partial\Omega$*, then the numerical fluxes defined by* (3.3) *and* (3.4) *satisfy*

$$\sum_{K\in\Omega_h}H_{\partial K}(u_h,w_h)=S(u_h)\geq 0,\tag{3.13}$$

where $S(\cdot)$ *is defined by* (3.12).

Proof. Firstly, we notice that

$$\sum_{K\in\Omega_h}H_{\partial K}(u_h,w_h)=\sum_{K\in\Omega_h}\Big(\sum_{e\in\mathscr{E}_h^I}H_{\partial K\cap e}(u_h,w_h)+\sum_{e\in\mathscr{E}_h^0}H_{\partial K\cap e}(u_h,w_h)\Big).\tag{3.14}$$

For any $e\in\mathscr{E}_h^I$, we suppose $e=\partial K_1\cap\partial K_2$, by (3.3), it is easy to check that

$$H_{\partial K_1\cap e}(u_h,w_h)+H_{\partial K_2\cap e}(u_h,w_h)=0,$$

hence,

$$\sum_{K\in\Omega_h}\sum_{e\in\mathscr{E}_h^I}H_{\partial K\cap e}(u_h,w_h)=0.\tag{3.15}$$

For $e\in\mathscr{E}_h^0$, without loss of generality, we assume $e\in\mathscr{E}_h^{0,b}$, i.e., e is the bottom boundary face of some element K_{i1}, $i\in\{1,2,\dots,N_x\}$. According to the definition of the boundary flux (3.4), we have

$$\widehat{u}\big|_e=\mathsf{P}_M\big(f_D\big)\big|_e=0,\quad \widehat{\nabla u}\cdot\boldsymbol{\nu}_b\big|_e=\mathsf{P}_M\big(f_N\big)\big|_e=0,\quad \widehat{w}\big|_e=w_h^+\big|_e,$$
$$\widehat{\nabla w}\cdot\boldsymbol{\nu}_b\big|_e=(\nabla w_h)^+\cdot\boldsymbol{\nu}_b\big|_e+\frac{k_4}{h^3}\Big(u_h^+-\mathsf{P}_M(f_D)\Big)\Big|_e=(\nabla w_h)^+\cdot\boldsymbol{\nu}_b\big|_e+\frac{k_4}{h^3}u_h^+\big|_e.$$

Therefore,

$$H_{\partial K_{i1}\cap e}(u_h,w_h)=\langle w_h^+,\nabla u_h^+\cdot\boldsymbol{\nu}_b\rangle_e-\langle u_h^+,\nabla w_h^+\cdot\boldsymbol{\nu}_b\rangle_e+\langle\nabla w_h^+\cdot\boldsymbol{\nu}_b,u_h^+\rangle_e$$

$$
\begin{aligned}
&- \langle w_h^+, \nabla u_h^+ \cdot \boldsymbol{\nu}_b \rangle_e + \frac{k_4}{h^3} \langle u_h^+, u_h^+ \rangle_e \\
=&\frac{k_4}{h^3} \int_{I_i} \Big(u_h\big(x, y_{\frac{1}{2}}^+\big) \Big)^2 \, dx.
\end{aligned}
$$

Similarly, we can derive that, for $i = 1, \ldots, N_x,\ j = 1, \ldots, N_y$,

$$
\begin{aligned}
H_{\partial K_{iN_y} \cap e}(u_h, w_h) =& \frac{k_2}{h} \int_{I_i} \Big((u_h)_y\big(x, y_{N_y+\frac{1}{2}}^-\big) \Big)^2 \, dx, \quad e \in \mathscr{E}_h^{0,t}, \\
H_{\partial K_{1j} \cap e}(u_h,\, w_h) =& \frac{k_3}{h^3} \int_{J_j} \Big(u_h\big(x_{\frac{1}{2}}^+, y\big) \Big)^2 \, dy, \qquad\quad e \in \mathscr{E}_h^{0,l}, \\
H_{\partial K_{N_x j} \cap e}(u_h, w_h) =& \frac{k_1}{h} \int_{J_j} \Big((u_h)_x\big(x_{N_x+\frac{1}{2}}^-, y\big) \Big)^2 \, dy, \quad e \in \mathscr{E}_h^{0,r}.
\end{aligned}
$$

Therefore, summing over $K \in \Omega_h$ and $e \in \mathscr{E}_h^0$, we obtain

$$
\sum_{K \in \Omega_h} \sum_{e \in \mathscr{E}_h^0} H_{\partial K \cap e}(u_h, w_h) = S(u_h). \tag{3.16}
$$

Since the penalty parameters $k_i > 0, i = 1, 2, 3, 4$, then (3.13) follows by (3.14), (3.15) and (3.16). □

Similar to Lemma 3.2, we have the following lemma for other three types of boundary conditions.

Lemma 3.3. *If the boundary conditions* (1.2b)–(1.2d) *are homogeneous, then the numerical fluxes defined by* (3.3) *and* (3.5)–(3.7) *satisfy*

$$
\sum_{K \in \Omega_h} H_{\partial K}(u_h, w_h) = 0.
$$

Theorem 3.4. *For the two-dimensional fourth-order equation* (1.1) *with the homogeneous boundary conditions in* (1.2a)–(1.2d)*, the UWLDG solutions* u_h, w_h *of the scheme* (3.2) *with the interior flux* (3.3) *and the corresponding boundary fluxes* (3.4)–(3.7) *satisfy*

$$
\frac{1}{2} \frac{d}{dt} \|u_h(t)\|^2 + \|w_h(t)\|^2 \le 0. \tag{3.17}
$$

Proof. Take $(p, q) = (u_h, w_h)$ and add the two equations in (3.2), then use integration by parts, we obtain

$$
\left((u_h)_t, u_h\right)_K + \left(w_h, w_h\right)_K + H_{\partial K}\left(u_h, w_h\right) = 0,\ \forall K \in \Omega_h,
$$

where $H_{\partial K}(\cdot, \cdot)$ is defined by (3.11). We sum over all the elements K in Ω_h to get

$$
\frac{1}{2} \frac{d}{dt} \|u_h(t)\|^2 + \|w_h(t)\|^2 + \sum_{K \in \Omega_h} H_{\partial K}(u_h, w_h) = 0.
$$

By Lemmas 3.2-3.3, we immediately arrive at the L^2-stability result (3.17). □

3.3. **Optimal error estimates.** In this subsection, we mainly consider optimal error estimates of the UWLDG scheme (3.2) with numerical fluxes (3.3)–(3.4) for solving the two-dimensional problem (1.1) with the Dirichlet B.C. (1.2a), since it is more involved. To this end, let us firstly introduce the semi-norm on the boundary: for $\forall v \in H^\ell(\Omega_h)$, $\ell \geq 2$,

$$\|v\|_{\partial K} := \left(\int_{J_j} \left[(v^-_{i+\frac{1}{2},y})^2 + (v^+_{i-\frac{1}{2},y})^2 \right] dy + \int_{I_i} \left[(v^-_{x,j+\frac{1}{2}})^2 + (v^+_{x,j-\frac{1}{2}})^2 \right] dx \right)^{\frac{1}{2}}.$$

Then, we denote $\|\nabla v\|_{\partial K} = \left(\|v_x\|^2_{\partial K} + \|v_y\|^2_{\partial K} \right)^{\frac{1}{2}}$, and for any subset $\widetilde{K} \subseteq \Omega_h$,

$$\|v\|_{\partial \widetilde{K}} = \Big(\sum_{K \in \widetilde{K}} \|v\|^2_{\partial K} \Big)^{\frac{1}{2}}, \ \|\nabla v\|_{\partial \widetilde{K}} = \Big(\sum_{K \in \widetilde{K}} \|\nabla v\|^2_{\partial K} \Big)^{\frac{1}{2}}, \ \|v\|_{\ell, \widetilde{K}} = \Big(\sum_{K \in \widetilde{K}} \|v\|^2_{\ell, K} \Big)^{\frac{1}{2}}.$$

The following trace and inverse inequalities [14] are useful in our analysis.

Lemma 3.5. *For any $v \in H^1(K)$, there exists a positive constant C, such that*

$$\|v\|^2_{\partial K} \leq C \|v\|_K \|v\|_{1,K},$$

where C is independent of the mesh size h.

Lemma 3.6. *For any $q \in \mathcal{Q}^k(K)$, there exist a positive constants C, such that*

$$\|q\|_{\partial K} \leq C h_K^{-\frac{1}{2}} \|q\|_K, \quad \|\nabla q\|_K \leq C h_K^{-1} \|q\|_K,$$

where $\|\nabla q\|_K = \left(\int_K \nabla q \cdot \nabla q \, d\boldsymbol{x} \right)^{\frac{1}{2}}$, C is independent of the mesh size h.

3.3.1. *Projection and its properties.* For two-dimensional Cartesian meshes, the projection can be constructed as the tensor product of one-dimensional projections. We define $\Pi : H^2(\Omega_h) \to W_h$ as

$$\Pi u := \mathsf{P}_{M_x} \otimes \mathsf{P}_{M_y} u, \tag{3.18}$$

where P_M is the one-dimensional projection given by (2.17a)–(2.17b), and the subscripts x and y indicate that the projection P_M is applied with respect to the corresponding variable. Specifically, for all $K_{ij} = I_i \times J_j = (x_{i-\frac{1}{2}}, x_{i+\frac{1}{2}}) \times (y_{j-\frac{1}{2}}, y_{j+\frac{1}{2}})$ and $\forall v_h \in \mathcal{Q}^{k-2}(K_{ij})$, Πu satisfies the following identities

$$\int_{K_{ij}} \Pi u(x,y) v_h(x,y) dx dy = \int_{K_{ij}} u(x,y) v_h(x,y) dx dy, \tag{3.19a}$$

$$\int_{I_i} \Pi u\big(x, y^+_{j-\frac{1}{2}}\big) v_h\big(x, y^+_{j-\frac{1}{2}}\big) dx = \int_{I_i} u\big(x, y_{j-\frac{1}{2}}\big) v_h\big(x, y^+_{j-\frac{1}{2}}\big) dx, \tag{3.19b}$$

$$\int_{J_j} \Pi u\big(x^+_{i-\frac{1}{2}}, y\big) v_h\big(x^+_{i-\frac{1}{2}}, y\big) dy = \int_{J_j} u\big(x_{i-\frac{1}{2}}, y\big) v_h\big(x^+_{i-\frac{1}{2}}, y\big) dy, \tag{3.19c}$$

$$\int_{I_i} \big(\Pi u\big)_y\big(x, y^-_{j+\frac{1}{2}}\big) v_h\big(x, y^-_{j+\frac{1}{2}}\big) dx = \int_{I_i} u_y\big(x, y_{j+\frac{1}{2}}\big) v_h\big(x, y^-_{j+\frac{1}{2}}\big) dx, \tag{3.19d}$$

$$\int_{J_j} \big(\Pi u\big)_x\big(x^-_{i+\frac{1}{2}}, y\big) v_h\big(x^-_{i+\frac{1}{2}}, y\big) dy = \int_{J_j} u_x\big(x_{i+\frac{1}{2}}, y\big) v_h\big(x^-_{i+\frac{1}{2}}, y\big) dy, \tag{3.19e}$$

$$\Pi u\big(x^+_{i-\frac{1}{2}}, y^+_{j-\frac{1}{2}}\big) = u\big(x_{i-\frac{1}{2}}, y_{j-\frac{1}{2}}\big), \tag{3.19f}$$

$$\big(\Pi u\big)_x\big(x^-_{i+\frac{1}{2}}, y^+_{j-\frac{1}{2}}\big) = u_x\big(x_{i+\frac{1}{2}}, y_{j-\frac{1}{2}}\big), \tag{3.19g}$$

$$(\Pi u)_y\big(x^+_{i-\frac12}, y^-_{j+\frac12}\big) = u_y\big(x_{i-\frac12}, y_{j+\frac12}\big), \tag{3.19h}$$

$$(\Pi u)_{xy}\big(x^-_{i+\frac12}, y^-_{j+\frac12}\big) = u_{xy}\big(x_{i+\frac12}, y_{j+\frac12}\big). \tag{3.19i}$$

Clearly, the following relationship between Π and P_M holds:

Proposition 3.7. *For $\forall K_{ij} \in \Omega_h$, on the boundary ∂K_{ij}, we have*

$$\Pi u(x^+_{i-\frac12}, y) = \mathsf{P}_{M_y}\big(u(x_{i-\frac12}, y)\big),\ (\Pi u)_x(x^-_{i+\frac12}, y) = \mathsf{P}_{M_y}\big(u_x(x_{i+\frac12}, y)\big),\ y \in J_j;$$

$$\Pi u(x, y^+_{j-\frac12}) = \mathsf{P}_{M_x}\big(u(x, y_{j-\frac12})\big),\ (\Pi u)_y(x, y^-_{j+\frac12}) = \mathsf{P}_{M_x}\big(u_y(x, y_{j+\frac12})\big),\ x \in I_i.$$

Using a similar argument as that in [29, Lemma 6.1], it is easy to check the existence and uniqueness of the projection Π, and we also have the following approximation property.

Lemma 3.8. *Assume $u \in H^s(\Omega_h)$, $s \geq 2$, then there exists a unique $\Pi u \in W_h$ satisfying* (3.19). *Moreover, there holds*

$$\|u - \Pi u\|_K + h^{\ell}\|u - \Pi u\|_{\ell,K} + h^{\frac12}\|u - \Pi u\|_{\partial K} \leq Ch^{min\{k+1,\, s\}}\|u\|_{s,K},$$

where $1 \leq \ell \leq min\{k+1, s\}$ is an integer and C is a constant independent of h.

3.3.2. *Main results.* We are now ready to state the error estimate result of the UWLDG scheme solving (1.1) with the Dirichlet B.C. (1.2a).

Theorem 3.9. *Let u be the exact solution of the fourth order equation* (1.1) *with the Dirichlet B.C.* (1.2a), *$w = \Delta u$; and assume u is smooth enough, e.g., $\|u\|_{k+5}$, $\|u_t\|_{k+1}$ are bounded uniformly for any time t. Let u_h, w_h be solutions of the UWLDG scheme* (3.2) *with numerical fluxes* (3.3)–(3.4). *For $k \geq 1$, we have*

$$\|u(t) - u_h(t)\| + \int_0^t \|w(\tau) - w_h(\tau)\|\, d\tau \leq Ch^{k+1}, \tag{3.20}$$

where C is a function of t to the power at most $\frac{3}{2}$, which is independent of h, and dependent on $\|u\|_{k+5}$, $\|u_t\|_{k+1}$.

The proof of Theorem 3.9 is divided into the following five steps:

Step 1. The error equation. As usual, we denote

$$e_u = u - u_h, \quad e_w = w - w_h.$$

Since the exact solution u and w satisfy the following weak formulation:

$$(u_t, p)_K + (w, \Delta p)_K + \langle \nabla w \cdot \mathbf{n}, p\rangle_{\partial K} - \langle w, \nabla p \cdot \mathbf{n}\rangle_{\partial K} = 0,$$
$$(w, q)_K - (u, \Delta q)_K - \langle \nabla u \cdot \mathbf{n}, q\rangle_{\partial K} + \langle u, \nabla q \cdot \mathbf{n}\rangle_{\partial K} = 0,$$

then we can get the cell error equation as

$$\big((e_u)_t, p\big)_K + (e_w, \Delta p)_K + \langle \widehat{\nabla e_w} \cdot \mathbf{n}, p\rangle_{\partial K} - \langle \widehat{e_w}, \nabla p \cdot \mathbf{n}\rangle_{\partial K} = 0, \tag{3.21a}$$

$$(e_w, q)_K - (e_u, \Delta q)_K - \langle \widehat{\nabla e_u} \cdot \mathbf{n}, q\rangle_{\partial K} + \langle \widehat{e_u}, \nabla q \cdot \mathbf{n}\rangle_{\partial K} = 0, \tag{3.21b}$$

where

$$\widehat{e_u} = u - \widehat{u}, \qquad \widehat{\nabla e_u} \cdot \mathbf{n} = (\nabla u - \widehat{\nabla u}) \cdot \mathbf{n},$$
$$\widehat{e_w} = w - \widehat{w}, \quad \widehat{\nabla e_w} \cdot \mathbf{n} = (\nabla w - \widehat{\nabla w}) \cdot \mathbf{n}.$$

Step 2. The error decomposition. Denote $e_u = \eta_u - \xi_u$, $e_w = \eta_w - \xi_w$ with

$$\eta_u = u - \Pi u,\ \xi_u = u_h - \Pi u, \quad \eta_w = w - \Pi w,\ \xi_w = w_h - \Pi w.$$

• At the interior face $e \in \mathscr{E}_h^I$, we naturally have

$$\begin{aligned} &\widehat{\eta_u}\big|_e = \eta_u^+\big|_e,\ \widehat{\xi_u}\big|_e = \xi_u^+\big|_e, \quad \widehat{\nabla\eta_u}\big|_e = (\nabla\eta_u)^-\big|_e,\ \widehat{\nabla\xi_u}\big|_e = (\nabla\xi_u)^-\big|_e, \\ &\widehat{\eta_w}\big|_e = \eta_w^+\big|_e,\ \widehat{\xi_w}\big|_e = \xi_w^+\big|_e, \quad \widehat{\nabla\eta_w}\big|_e = (\nabla\eta_w)^-\big|_e, \widehat{\nabla\xi_w}\big|_e = (\nabla\xi_w)^-\big|_e. \end{aligned} \tag{3.22}$$

• At the boundary face $e \in \mathscr{E}_h^0$, we specially let

$$\widehat{\eta_u}\big|_e := \widehat{e_u}\big|_e, \quad \widehat{\xi_u}\big|_e := 0, \quad \forall e \in \mathscr{E}_h^0, \tag{3.23a}$$

$$\widehat{\nabla\eta_u}\cdot\boldsymbol{\nu}_m\big|_e := \widehat{\nabla e_u}\cdot\boldsymbol{\nu}_m\big|_e, \quad \widehat{\nabla\xi_u}\cdot\boldsymbol{\nu}_m\big|_e := 0, \quad \forall e \in \mathscr{E}_h^{0,m}, m = l, b, r, t, \tag{3.23b}$$

$$\begin{aligned} &\widehat{\eta_w}\big|_e := \eta_w^+\big|_e, \quad \widehat{\xi_w}\big|_e := \xi_w^+\big|_e, \quad \forall e \in \mathscr{E}_h^{0,l}, \mathscr{E}_h^{0,b}, \\ &\widehat{\eta_w}\big|_e := \eta_w^-\big|_e, \quad \widehat{\xi_w}\big|_e := \xi_w^-\big|_e + \frac{k_1}{h}\left[\!\left[(u_h)_x\right]\!\right]\big|_e, \quad \forall e \in \mathscr{E}_h^{0,r}, \\ &\widehat{\eta_w}\big|_e := \eta_w^-\big|_e, \quad \widehat{\xi_w}\big|_e := \xi_w^-\big|_e + \frac{k_2}{h}\left[\!\left[(u_h)_y\right]\!\right]\big|_e, \quad \forall e \in \mathscr{E}_h^{0,t}, \end{aligned} \tag{3.23c}$$

(3.23d)

$$\widehat{\nabla\eta_w}\cdot\boldsymbol{\nu}_l\big|_e := (\nabla\eta_w)^+\cdot\boldsymbol{\nu}_l\big|_e, \quad \widehat{\nabla\xi_w}\cdot\boldsymbol{\nu}_l\big|_e := (\nabla\xi_w)^+\cdot\boldsymbol{\nu}_l\big|_e + \frac{k_3}{h^3}\left[\!\left[u_h\right]\!\right]\big|_e, \ \forall e \in \mathscr{E}_h^{0,l},$$

$$\widehat{\nabla\eta_w}\cdot\boldsymbol{\nu}_b\big|_e := (\nabla\eta_w)^+\cdot\boldsymbol{\nu}_b\big|_e, \ \widehat{\nabla\xi_w}\cdot\boldsymbol{\nu}_b\big|_e := (\nabla\xi_w)^+\cdot\boldsymbol{\nu}_b\big|_e + \frac{k_4}{h^3}\left[\!\left[u_h\right]\!\right]\big|_e, \ \forall e \in \mathscr{E}_h^{0,b},$$

$$\widehat{\nabla\eta_w}\cdot\boldsymbol{\nu}_m\big|_e := (\nabla\eta_w)^-\cdot\boldsymbol{\nu}_m\big|_e, \ \widehat{\nabla\xi_w}\cdot\boldsymbol{\nu}_m\big|_e := (\nabla\xi_w)^-\cdot\boldsymbol{\nu}_m\big|_e, \ \forall e \in \mathscr{E}_h^{0,m}, m = r, t.$$

Based on the above decomposition, for all $K \in \Omega_h$, we have

$$\begin{aligned} &\widehat{e_u}\big|_{\partial K} = \widehat{\eta_u}\big|_{\partial K} - \widehat{\xi_u}\big|_{\partial K}, \quad \widehat{\nabla e_u}\cdot\mathbf{n}\big|_{\partial K} = \widehat{\nabla\eta_u}\cdot\mathbf{n}\big|_{\partial K} - \widehat{\nabla\xi_u}\cdot\mathbf{n}\big|_{\partial K}, \\ &\widehat{e_w}\big|_{\partial K} = \widehat{\eta_w}\big|_{\partial K} - \widehat{\xi_w}\big|_{\partial K}, \ \widehat{\nabla e_w}\cdot\mathbf{n}\big|_{\partial K} = \widehat{\nabla\eta_w}\cdot\mathbf{n}\big|_{\partial K} - \widehat{\nabla\xi_w}\cdot\mathbf{n}\big|_{\partial K}. \end{aligned}$$

Hence, we can decompose the cell error equation (3.21) into the following form

$$\begin{aligned} \big((\xi_u)_t, p\big)_K + B_K\left(\xi_w, p\right) &= \big((\eta_u)_t, p\big)_K + B_K\left(\eta_w, p\right), \\ \left(\xi_w, q\right)_K - B_K\left(\xi_u, q\right) &= \left(\eta_w, q\right)_K - B_K\left(\eta_u, q\right), \end{aligned} \tag{3.24}$$

where $B_K(\cdot,\cdot)$ is defined by (3.8). Now, we take $p = \xi_u$, $q = \xi_w$ and add the two equations in (3.24), after summing over K, we obtain,

$$\big((\xi_u)_t, \xi_u\big)_{\Omega_h} + (\xi_w, \xi_w)_{\Omega_h} + \Lambda_1 = \big((\eta_u)_t, \xi_u\big)_{\Omega_h} + (\eta_w, \xi_w)_{\Omega_h} + \Lambda_2, \tag{3.25}$$

where

$$\Lambda_1 = \sum_{K\in\Omega_h}\Big(B_K(\xi_w,\xi_u) - B_K(\xi_u,\xi_w)\Big), \quad \Lambda_2 = \sum_{K\in\Omega_h}\Big(B_K(\eta_w,\xi_u) - B_K(\eta_u,\xi_w)\Big).$$

Step 3. The estimate of Λ_1. The estimate of Λ_1 is given in the following lemma.

Lemma 3.10. *$\Lambda_1 = S(\xi_u)$, where $S(\cdot)$ is defined by* (3.12).

Proof. Firstly, for $\forall K \in \Omega_h$, using integration by parts, we obtain

$$\Lambda_1 = \sum_{K\in\Omega_h}\Big(B_K(\xi_w,\xi_u) - B_K(\xi_u,\xi_w)\Big) = \sum_{K\in\Omega_h}\widetilde{H}_{\partial K}(\xi_u,\xi_w),$$

where

$$\begin{aligned} \widetilde{H}_{\partial K}(\xi_u,\xi_w) = &\langle\xi_w, \nabla\xi_u\cdot\mathbf{n}\rangle_{\partial K} - \langle\xi_u, \nabla\xi_w\cdot\mathbf{n}\rangle_{\partial K} + \langle\widehat{\nabla\xi_w}\cdot\mathbf{n}, \xi_u\rangle_{\partial K} \\ &- \langle\widehat{\xi_w}, \nabla\xi_u\cdot\mathbf{n}\rangle_{\partial K} - \langle\widehat{\nabla\xi_u}\cdot\mathbf{n}, \xi_w\rangle_{\partial K} + \langle\widehat{\xi_u}, \nabla\xi_w\cdot\mathbf{n}\rangle_{\partial K}. \end{aligned} \tag{3.26}$$

In addition, the property of projection Π in Proposition 3.7 implies that

$$\mathsf{P}_{M_y}\big(u|_e\big) = (\Pi u)^+|_e,\ e \in \mathscr{E}_h^{0,l}, \quad \mathsf{P}_{M_y}(u_x|_e) = \big((\Pi u)_x\big)^-|_e,\ e \in \mathscr{E}_h^{0,r},$$
$$\mathsf{P}_{M_x}\big(u|_e\big) = (\Pi u)^+|_e,\ e \in \mathscr{E}_h^{0,b}, \quad \mathsf{P}_{M_x}(u_y|_e) = \big((\Pi u)_y\big)^-|_e,\ e \in \mathscr{E}_h^{0,t},$$

which allows us to rewrite those terms with penalty in (3.23c)–(3.23d) as

$$\widehat{\xi_w}\big|_e = \xi_w^-\big|_e - \frac{k_1}{h}\big((\xi_u)_x\big)^-\big|_e,\ e \in \mathscr{E}_h^{0,r},$$
$$\widehat{\xi_w}\big|_e = \xi_w^-\big|_e - \frac{k_2}{h}\big((\xi_u)_y\big)^-\big|_e,\ e \in \mathscr{E}_h^{0,t},$$
$$\widehat{\nabla\xi_w}\cdot\boldsymbol{\nu}_l\big|_e = \big(\nabla\xi_w\big)^+\cdot\boldsymbol{\nu}_l\big|_e + \frac{k_3}{h^3}\xi_u^+\big|_e,\ e \in \mathscr{E}_h^{0,l},$$
$$\widehat{\nabla\xi_w}\cdot\boldsymbol{\nu}_b\big|_e = \big(\nabla\xi_w\big)^+\cdot\boldsymbol{\nu}_b\big|_e + \frac{k_4}{h^3}\xi_u^+\big|_e,\ e \in \mathscr{E}_h^{0,b}.$$

Next, using a similar argument as that in the proof of (3.13), we can obtain

$$\sum_{K\in\Omega_h}\widetilde{H}_{\partial K}(\xi_u,\xi_w) = S(\xi_u).$$

This completes the proof of this lemma. □

Step 4. The estimate of Λ_2. The following polynomials preserving properties of degree up to $k+2$ is crucial for the estimates of Λ_2, we list them in the following Lemmas 3.11–3.12.

Lemma 3.11. *If $w \in \mathcal{P}^{k+2}$ $(k \geq 1)$, $p \in W_h$, we have*

$$B_K(\eta_w, p) = 0,\ \forall K \in \Omega_h^I, \tag{3.27a}$$

(3.27b)

$$\sum_{K\in\Omega_h^0} B_K(\eta_w,p) = -\sum_{i=1}^{N_x}\int_{I_i}\Big(\eta_w\big(x,y^-_{N_y+\frac{1}{2}}\big)p_y\big(x,y^-_{N_y+\frac{1}{2}}\big) + (\eta_w)_y\big(x,y^+_{\frac{1}{2}}\big)p\big(x,y^+_{\frac{1}{2}}\big)\Big)dx$$
$$-\sum_{j=1}^{N_y}\int_{J_j}\Big(\eta_w\big(x^-_{N_x+\frac{1}{2}},y\big)p_x\big(x^-_{N_x+\frac{1}{2}},y\big) + (\eta_w)_x\big(x^+_{\frac{1}{2}},y\big)p\big(x^+_{\frac{1}{2}},y\big)\Big)dy.$$

Proof. The proof of this lemma is provided in Appendix A.1. □

Lemma 3.12. *If $u \in \mathcal{P}^{k+2}$ $(k \geq 1)$, $q \in W_h$, we have*

$$B_K(\eta_u, q) = 0,\ \forall K \in \Omega_h. \tag{3.28}$$

Proof. The proof of this lemma is provided in Appendix A.2. □

By Lemmas 3.11–3.12, we can obtain a superconvergent property of $B_K(\eta_w, p)$ and $B_K(\eta_u, q)$ and show it in Lemmas 3.13 and 3.14, respectively.

Lemma 3.13. *For $p \in W_h$ and $k \geq 1$, we have*

$$\sum_{K\in\Omega_h}|B_K(\eta_w,p)| \leq Ch^{k+1}\|w\|_{k+3}\|p\| + Ch^{2k+2}\|w\|_{k+1}^2 + \frac{1}{2}S(p), \tag{3.29}$$

where C is a constant independent of the mesh size h.

Proof. The proof of this lemma is provided in Appendix A.3. □

Lemma 3.14. *For $q \in W_h$ and $k \geq 1$, we have*

$$\sum_{K\in\Omega_h} |B_K(\eta_u, q)| \leq Ch^{k+1}\|u\|_{k+5}\|q\|, \tag{3.30}$$

where C is a constant independent of the mesh size h.

Proof. The proof of this lemma is provided in Appendix A.4. □

Lemma 3.15. *For Λ_2, we have*

$$|\Lambda_2| \leq Ch^{k+1}\|\xi_u\| + Ch^{k+1}\|\xi_w\| + Ch^{2k+2} + \frac{1}{2}S(\xi_u), \tag{3.31}$$

where C depends on $\|u\|_{k+5}$, but is independent of the mesh size h.

Proof. Taking $p = \xi_u$, $q = \xi_w$ in Lemma 3.13 and Lemma 3.14, respectively, we can immediately get (3.31). □

Step 5. The proof of Theorem 3.9.

Proof. Recalling the error equation (3.25), and using the Cauchy–Schwarz inequality and approximation property of the projection Π in Lemma 3.8, we arrive at

$$\frac{1}{2}\frac{d}{dt}\|\xi_u(t)\|^2 + \|\xi_w(t)\|^2 + \Lambda_1 \leq Ch^{k+1}\|\xi_u(t)\| + Ch^{k+1}\|\xi_w(t)\| + |\Lambda_2|.$$

By Lemma 3.10 and Lemma 3.15, we immediately obtain

$$\frac{1}{2}\frac{d}{dt}\|\xi_u(t)\|^2 + \|\xi_w(t)\|^2 \leq Ch^{k+1}\|\xi_u(t)\| + Ch^{k+1}\|\xi_w(t)\| + Ch^{2k+2}.$$

Then, using the same technique as that in the proof of Theorem 2.5 for the one-dimensional case, we get

$$\|\xi_u(t)\| + \int_0^t \|\xi_w(\tau)\|\, d\tau \leq Ch^{k+1},$$

and hence

$$\|e_u(t)\| + \int_0^t \|e_w(\tau)\|\, d\tau \leq Ch^{k+1},$$

where C is a function of t of power at most $\frac{3}{2}$, which depends on $\|u\|_{k+5}$, $\|u_t\|_{k+1}$, but is independent of h. □

Remark 3.16. For the fourth-order problem (1.1) with the G-Dirichlet B.C. (1.2b), for $k \geq 2$, we can derive the optimal error estimate (3.20) for the UWLDG scheme (3.2) with numerical fluxes (3.3) and (3.5) by using the projection $\mathsf{P}_{N_x} \otimes \mathsf{P}_{N_y}$.

Remark 3.17. For the fourth-order problem (1.1) with the Neumann B.C. (1.2c) and the mixed B.C. (1.2d), when the UWLDG scheme (3.2) with numerical fluxes (3.3), (3.6) and (3.7) are considered, the optimal error estimates in (3.20) for $k \geq 1$ can also be derived by using the projection $\mathsf{P}_{D_x} \otimes \mathsf{P}_{D_y}$ and $\mathsf{P}_{M_x} \otimes \mathsf{P}_{M_y}$, respectively.

4. Numerical examples

In this section, to confirm the theoretical convergence results of the UWLDG method, we present several numerical examples for one- and two-dimensional time-dependent linear fourth-order initial-boundary value problems. Noting that the theoretical results mainly concentrate on the h-version convergence and smooth solutions in this work, we numerically test the p-version case and the problem with singularities in an L-shape domain. In all experiments, we use the four-stage singly diagonally implicit Runge–Kutta method with third order of accuracy (SDIRK3) for time discretization with final time $T = 1$.

Example 4.1. Consider the one-dimensional linear fourth order problem

$$u_t + u_{xxxx} = 0,\ u(x,0) = \sin(x), \quad (x,t) \in [0, 2\pi] \times (0, T],$$

with boundary conditions as in (2.2a)–(2.2d) such that the exact solution is

$$u(x,t) = e^{-t}\sin(x).$$

For the Dirichlet B.C. (2.2a), our computation is based on the flux (2.4)–(2.5). Table 4.1 lists the L^2 errors and orders for e_u, e_w using numerical fluxes with and without penalties for $\mathcal{P}^k$ polynomials ($1 \le k \le 3$). It is observed that, for the case with penalty terms (the penalty parameters $k_1 = k_2 = 1$), the errors achieve optimal $(k+1)$th order accuracy for both $\|e_u\|$ and $\|e_w\|$, which is consistent with Theorem 2.5. For the case without penalties ($k_1 = k_2 = 0$), loss of order for $\|e_u\|$ is observed, especially for $k = 2$, order lost up to one and a half, which indicates that the penalty terms are necessary for both theoretical analysis and numerical implementation.

Table 4.1. L^2 errors $\|e_u\|$, $\|e_w\|$ and orders for Example 4.1 with the Dirichlet B.C. with and without penalties using $\mathcal{P}^k$ polynomials on a uniform mesh of N cells.

	N	with penalty				without penalty			
		$\|e_u\|$	order	$\|e_w\|$	order	$\|e_u\|$	order	$\|e_w\|$	order
$\mathcal{P}^1$	10	5.67E-02	–	4.37E-02	–	9.22E-02	–	4.95E-02	–
	20	1.35E-02	1.87	1.14E-02	1.93	2.99E-02	1.62	1.19E-02	2.05
	40	3.93E-03	1.97	2.85E-03	2.00	9.87E-03	1.60	2.89E-03	2.04
	80	9.87E-04	1.99	7.14E-04	2.00	3.35E-03	1.55	7.16E-04	2.01
	160	2.47E-04	1.99	1.78E-04	2.00	1.15E-03	1.53	1.78E-04	2.00
	320	6.18E-05	1.99	4.46E-05	2.00	4.05E-04	1.51	4.46E-05	2.00
$\mathcal{P}^2$	10	8.54E-04	–	8.05E-04	–	4.34E-02	–	1.62E-03	–
	20	9.73E-05	3.13	9.92E-05	3.02	1.59E-02	1.44	1.66E-04	3.28
	40	1.23E-05	2.98	1.23E-05	3.00	5.68E-03	1.48	1.71E-05	3.27
	80	1.53E-06	2.99	1.53E-06	3.00	2.01E-03	1.49	1.89E-06	3.20
	160	1.92E-07	3.00	1.92E-07	3.00	7.12E-04	1.49	2.13E-07	3.12
	320	2.40E-08	3.00	2.40E-08	3.00	2.51E-04	1.49	2.53E-08	3.07
$\mathcal{P}^3$	10	2.25E-05	–	2.19E-05	–	9.86E-04	–	2.31E-05	–
	20	1.37E-06	4.03	1.37E-06	3.99	8.85E-05	3.47	1.38E-06	4.06
	40	8.59E-08	3.99	8.59E-08	3.99	7.85E-06	3.49	8.60E-08	4.01
	80	5.37E-09	3.99	5.37E-09	3.99	6.94E-07	3.49	5.37E-09	4.00
	160	3.35E-10	3.99	3.35E-10	3.99	6.14E-08	3.49	3.35E-10	4.00
	320	2.09E-11	3.99	2.09E-11	3.99	5.42E-09	3.49	2.09E-11	4.00

For the G-Dirichlet, Neumann and mixed boundary conditions in (2.2b)–(2.2d), our computation is based on the flux choice (2.4) and (2.6)–(2.8). The errors $\|e_u\|$,

$\|e_w\|$ and numerical orders are shown in Tables 4.2 and 4.3 respectively, which display the expected optimal $(k+1)$th convergence rates except for the case of the G-Dirichlet B.C. with $\mathcal{P}^1$ polynomials. This agrees with our theoretical results discussed in Remarks 2.6 and 2.7.

TABLE 4.2. L^2 errors $\|e_u\|$ and orders for Example 4.1 with the G-Dirichlet, Neumann and mixed boundary conditions using $\mathcal{P}^k$ polynomials on a uniform mesh of N cells.

	N	G-Dirichlet B.C.		Neumann B.C.		mixed B.C.	
		$\|e_u\|$	order	$\|e_u\|$	order	$\|e_u\|$	order
$\mathcal{P}^1$	10	9.94E-02	–	3.41E-02	–	5.10E-02	–
	20	2.89E-02	1.77	9.21E-03	1.88	1.34E-02	1.92
	40	9.05E-03	1.67	2.35E-03	1.96	3.40E-03	1.98
	80	2.98E-03	1.59	5.92E-04	1.99	8.53E-04	1.99
	160	1.01E-03	1.55	1.48E-04	1.99	2.13E-04	1.99
	320	3.53E-04	1.52	3.70E-05	1.99	5.33E-05	1.99
$\mathcal{P}^2$	10	1.08E-03	–	7.45E-04	–	8.06E-04	–
	20	1.19E-04	3.18	9.52E-05	2.96	9.91E-05	3.02
	40	1.36E-05	3.12	1.20E-05	2.97	1.23E-05	3.00
	80	1.62E-06	3.07	1.52E-06	2.98	1.53E-06	3.00
	160	1.97E-07	3.03	1.91E-07	2.99	1.92E-07	3.00
	320	2.43E-08	3.02	2.39E-08	2.99	2.40E-08	3.00
$\mathcal{P}^3$	10	2.22E-05	–	2.18E-05	–	2.19E-05	–
	20	1.37E-06	4.01	1.37E-06	3.99	1.37E-06	3.99
	40	8.59E-08	4.00	8.59E-08	3.99	8.59E-08	3.99
	80	5.37E-09	4.00	5.37E-09	3.99	5.37E-09	3.99
	160	3.35E-10	3.99	3.35E-10	3.99	3.35E-10	3.99
	320	2.09E-11	3.99	2.09E-11	3.99	2.09E-11	3.99

Although a theoretical analysis of the convergence concerning polynomial degree k is not provided, we numerically tested p-version of our scheme for Example 4.1 with four types of boundary conditions. We take the grid number $N = 20$ and calculate the L^2 error of e_u, e_w for $\mathcal{P}^k$ $(k = 1, \ldots, 8)$ polynomials. The relationship between the logarithmic scale of the error $\|e_u\|$, $\|e_w\|$ and the polynomial degrees is shown in Figures 4.1–4.2, from which we can clearly see that the errors decay exponentially with respect to k.

Example 4.2. Consider the following two-dimensional fourth-order problem

$$u_t + \Delta^2 u = 0, \ \ u(x, y, 0) = \sin(x + y), \ \ (x, y) \in [0, 2\pi] \times [0, 2\pi], t \in (0, T],$$

equipped with boundary conditions (1.2a)–(1.2d) such that the exact solution is

$$u(x, y, t) = e^{-4t} \sin(x + y).$$

We compute this example using the interior numerical flux (3.3) and boundary fluxes (3.4)–(3.7) for corresponding boundary conditions.

In Table 4.4, we list the computation results for the Dirichlet B.C. (1.2a). We observe that the UWLDG scheme with penalty terms gives the optimal $(k+1)$th order of the accuracy, which is consistent with Theorem 3.9. Here, the penalty parameters are chosen as $k_i = 1$, $i = 1, 2, 3, 4$. Moreover, if we remove the penalty

TABLE 4.3. L^2 errors $\|e_w\|$ and orders for Example 4.1 with the G-Dirichlet, Neumann and mixed boundary conditions using $\mathcal{P}^k$ polynomials on a uniform mesh of N cells.

	N	G-Dirichlet B.C.		Neumann B.C.		mixed B.C.	
		$\|e_w\|$	order	$\|e_w\|$	order	$\|e_w\|$	order
$\mathcal{P}^1$	10	6.15E-02	–	3.08E-02	–	3.75E-02	–
	20	1.65E-02	1.89	8.39E-03	1.87	9.65E-03	1.95
	40	5.17E-03	1.67	2.14E-03	1.97	2.40E-03	2.00
	80	1.72E-03	1.58	5.38E-04	1.99	6.01E-04	2.00
	160	5.89E-04	1.54	1.34E-04	1.99	1.50E-04	2.00
	320	2.05E-04	1.52	3.36E-05	1.99	3.75E-05	2.00
$\mathcal{P}^2$	10	1.04E-03	–	7.43E-04	–	7.93E-04	–
	20	1.18E-04	3.14	9.51E-05	2.96	9.86E-05	3.00
	40	1.36E-05	3.11	1.20E-05	2.97	1.23E-05	3.00
	80	1.62E-06	3.06	1.52E-06	2.98	1.53E-06	3.00
	160	1.97E-07	3.03	1.91E-07	2.99	1.92E-07	3.00
	320	2.43E-08	3.02	2.39E-08	2.99	2.40E-08	3.00
$\mathcal{P}^3$	10	2.22E-05	–	2.18E-05	–	2.19E-05	–
	20	1.37E-06	4.01	1.37E-06	3.99	1.37E-06	3.99
	40	8.59E-08	4.00	8.59E-08	3.99	8.59E-08	3.99
	80	5.37E-09	4.00	5.37E-09	3.99	5.37E-09	3.99
	160	3.35E-10	3.99	3.35E-10	3.99	3.35E-10	3.99
	320	2.09E-11	3.99	2.09E-11	3.99	2.09E-11	3.99

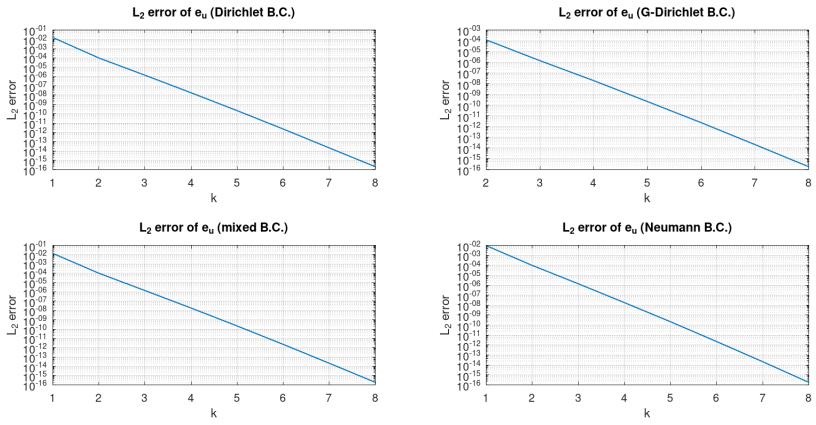

FIGURE 4.1. The error of $\|e_u\|$ in logarithmic scale with respect to polynomial degree k for different boundary conditions.

terms in the scheme, it is observed that at least one and a half order is lost for both $\|e_u\|$ and $\|e_w\|$.

In Tables 4.5 and 4.6, we show the approximation results of $\|e_u\|$ and $\|e_w\|$ for other three kinds of boundary conditions. We can observe the expected optimal convergence rates for the Neumann B.C. and mixed B.C. when $k = 1, 2$ and for

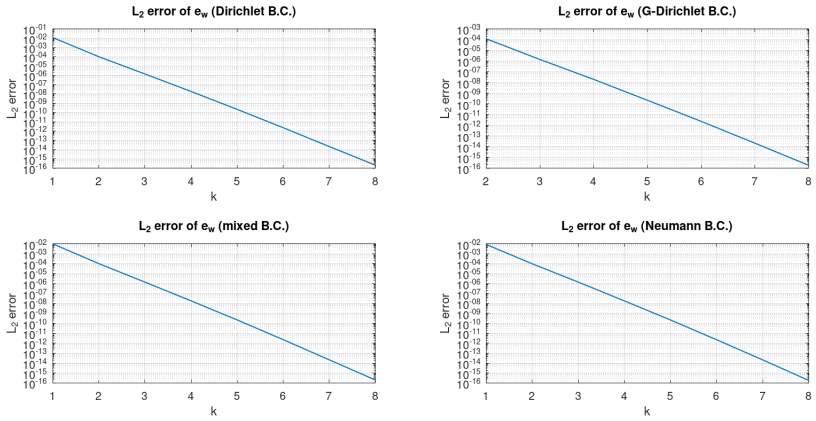

FIGURE 4.2. The error of $\|e_w\|$ in logarithmic scale with respect to polynomial degree k for different boundary conditions.

TABLE 4.4. L^2 errors $\|e_u\|$, $\|e_w\|$ and orders for Example 4.2 with the Dirichlet B.C., with and without penalties using $\mathcal{Q}^k$ polynomials on a uniform mesh of $N \times N$ cells.

	$N \times N$	with penalty				without penalty			
		$\|e_u\|$	order	$\|e_w\|$	order	$\|e_u\|$	order	$\|e_w\|$	order
$\mathcal{Q}^1$	10×10	9.39E-03	–	1.69E-02	–	5.50E-02	–	3.00E-02	–
	20×20	3.03E-03	1.62	5.52E-03	1.61	5.81E-02	-0.07	5.03E-02	-0.74
	40×40	8.06E-04	1.91	1.46E-03	1.92	6.05E-02	-0.05	4.39E-02	0.19
	60×60	3.56E-04	2.01	6.46E-04	2.01	5.73E-02	0.13	3.59E-02	0.49
	80×80	1.98E-04	2.03	3.60E-04	2.03	5.38E-02	0.22	3.00E-02	0.61
$\mathcal{Q}^2$	10×10	9.14E-05	–	1.75E-04	–	2.96E-02	–	9.28E-03	–
	20×20	7.60E-06	3.58	1.63E-05	3.42	1.13E-02	1.39	2.16E-03	2.10
	40×40	8.93E-07	3.08	1.83E-06	3.15	4.18E-03	1.43	6.21E-04	1.79
	60×60	2.61E-07	3.02	5.32E-07	3.05	2.32E-03	1.45	3.01E-04	1.78
	80×80	1.10E-07	3.01	2.22E-07	3.03	1.52E-03	1.46	1.82E-04	1.74

the G-Dirichlet B.C. when $k = 2$, which confirm our theoretical results discussed in Remarks 3.16 and 3.17.

It is worth pointing out that, the results listed in Tables 4.5 and 4.6 for the G-Dirichlet B.C. with $\mathcal{Q}^1$ polynomials are obtained by using the exact boundary conditions to define the boundary numerical flux $\widehat{u}$ and $\widehat{w}$, i.e., $\widehat{u}|_e = f_D|_e$, $\widehat{w}|_e = g_D|_e$, since the projection P_N does not exist when $k = 1$ and thus we cannot construct the numerical flux as (3.5). However, we can clearly see that about one and a half order is lost for both $\|e_u\|$ and $\|e_w\|$.

To further illustrate the special choice of the numerical boundary conditions is necessary in our implementation, here we show a "negative" example with "wrong" numerical fluxes on the boundary. We test again the Example 4.2 for four types of boundary conditions by choosing the standard L^2 projection of exact boundary conditions to replace the projection P_M, P_N, and P_D in the boundary fluxes (3.4)–(3.7). The approximation results are shown in Tables 4.7 and 4.8, from which we

can observe the loss of order, even to the extent of negative order, when the meshes are refined, especially for the case of the G-Dirichlet B.C. and the mixed B.C.

TABLE 4.5. L^2 errors $\|e_u\|$ and orders for Example 4.2 with the G-Dirichlet, Neumann and mixed boundary conditions using $\mathcal{Q}^k$ polynomials on a uniform mesh of $N \times N$ cells.

	$N \times N$	G-Dirichlet B.C.		Neumann B.C.		mixed B.C.	
		$\|e_u\|$	order	$\|e_u\|$	order	$\|e_u\|$	order
$\mathcal{Q}^1$	10×10	9.18E-02	–	3.23E-02	–	2.57E-02	–
	20×20	7.27E-02	0.33	9.90E-03	1.70	8.18E-03	1.65
	40×40	5.42E-02	0.42	2.62E-03	1.91	2.18E-03	1.90
	60×60	4.50E-02	0.45	1.18E-03	1.96	9.88E-04	1.95
	80×80	3.38E-02	0.50	6.68E-04	1.98	5.61E-04	1.96
$\mathcal{Q}^2$	10×10	1.08E-04	–	1.11E-04	–	1.17E-04	–
	20×20	9.36E-06	3.52	9.29E-06	3.58	9.40E-06	3.64
	40×40	9.81E-07	3.25	9.52E-07	3.28	9.58E-07	3.29
	60×60	2.77E-07	3.11	2.69E-07	3.11	2.70E-07	3.11
	80×80	1.14E-07	3.07	1.11E-07	3.05	1.12E-07	3.05

TABLE 4.6. L^2 errors $\|e_w\|$ and orders for Example 4.2 with the G-Dirichlet, Neumann and mixed boundary conditions using $\mathcal{Q}^k$ polynomials on a uniform mesh of $N \times N$ cells.

	$N \times N$	G-Dirichlet B.C.		Neumann B.C.		mixed B.C.	
		$\|e_w\|$	order	$\|e_w\|$	order	$\|e_w\|$	order
$\mathcal{Q}^1$	10×10	7.48E-02	–	4.27E-02	–	3.12E-02	–
	20×20	6.95E-02	0.11	1.25E-02	1.76	9.74E-03	1.68
	40×40	5.16E-02	0.42	3.29E-03	1.93	2.57E-03	1.92
	60×60	4.25E-02	0.48	1.47E-03	1.97	1.15E-03	1.97
	80×80	3.69E-02	0.49	8.33E-04	1.98	6.52E-04	1.98
$\mathcal{Q}^2$	10×10	1.73E-04	–	1.64E-04	–	1.61E-04	–
	20×20	1.70E-05	3.34	1.58E-05	3.37	1.58E-06	3.35
	40×40	1.90E-06	3.15	1.80E-06	3.13	1.81E-07	3.12
	60×60	5.47E-07	3.07	5.25E-07	3.04	5.27E-07	3.04
	80×80	2.27E-07	3.04	2.20E-07	3.02	2.21E-07	3.02

Example 4.3. To illustrate the capacity of the UWLDG method for problems with singularities, consider the following two-dimensional fourth-order problem in an L-shape domain $\Omega = [0, 2\pi]^2 \backslash \{(\pi, \pi]^2\}$,

$$u_t + \Delta^2 u = 0, \ (x, y) \in \Omega, \ t \in (0, T], \tag{4.1a}$$

with an initial condition

$$u(x, y, 0) = \sin(x + y), \tag{4.1b}$$

and the homogeneous Dirichlet B.C.

$$u = 0, \qquad \frac{\partial u}{\partial \boldsymbol{\nu}} = 0, \quad \text{on } \partial\Omega. \tag{4.1c}$$

TABLE 4.7. L^2 errors $\|e_u\|$ and orders for Example 4.2 with four types of boundary conditions using $\mathcal{Q}^k$ polynomials on a uniform mesh of $N \times N$ cells. Take the L^2 projection of exact boundary condition as boundary flux.

	$N \times N$	Dirichlet B.C.		G-Dirichlet B.C.		Neumann B.C.		mixed B.C.	
		$\|e_u\|$	order	$\|e_u\|$	order	$\|e_u\|$	order	$\|e_u\|$r	order
$\mathcal{Q}^1$	10×10	1.00E-03	–	6.86E-02	–	4.20E-02	–	4.33E-02	–
	20×20	3.09E-03	1.69	6.79E-02	0.01	1.31E-02	1.67	1.22E-02	1.82
	40×40	8.21E-04	1.91	5.33E-02	0.35	3.51E-03	1.90	3.13E-03	1.96
	60×60	3.63E-04	2.01	4.47E-02	0.43	1.58E-03	1.96	1.41E-03	1.96
	80×80	2.02E-04	2.03	3.87E-02	0.49	8.97E-04	1.97	8.10E-04	1.93
$\mathcal{Q}^2$	10×10	9.43E-05	–	2.81E-04	–	1.62E-04	–	1.10E-03	–
	20×20	8.02E-06	3.55	1.11E-05	4.65	1.18E-05	3.76	1.69E-04	2.69
	40×40	9.20E-07	3.12	1.04E-05	0.09	1.05E-06	3.48	1.72E-06	6.61
	60×60	2.77E-07	2.95	8.20E-07	6.26	2.90E-07	3.19	4.38E-07	3.38
	80×80	1.17E-07	2.99	7.91E-06	-7.87	1.43E-07	2.45	5.13E-07	-0.55

TABLE 4.8. L^2 errors $\|e_w\|$ and orders for Example 4.2 with four types of boundary conditions using $\mathcal{Q}^k$ polynomials on a uniform mesh of $N \times N$ cells. Take the L^2 projection of exact boundary condition as boundary flux.

	$N \times N$	Dirichlet B.C.		G-Dirichlet B.C.		Neumann B.C.		mixed B.C.	
		$\|e_w\|$	order	$\|e_w\|$	order	$\|e_w\|$	order	$\|e_w\|$	order
$\mathcal{Q}^1$	10×10	1.85E-02	–	5.99E-02	–	5.60E-02	–	4.54E-02	–
	20×20	5.66E-03	1.71	6.49E-02	-0.11	1.65E-02	1.76	1.32E-03	1.78
	40×40	1.49E-03	1.92	5.07E-02	0.35	4.33E-03	1.93	3.43E-03	1.94
	60×60	7.07E-04	1.83	4.21E-02	0.45	1.94E-03	1.97	1.54E-03	1.97
	80×80	3.73E-04	2.22	3.67E-02	0.47	1.10E-03	1.98	8.97E-04	1.88
$\mathcal{Q}^2$	10×10	2.12E-04	–	2.51E-04	–	2.13E-04	–	3.90E-04	–
	20×20	3.97E-05	2.41	1.92E-05	3.70	1.81E-05	3.55	1.21E-04	1.68
	40×40	1.52E-05	1.38	2.04E-05	-0.08	1.88E-06	3.26	4.54E-06	4.74
	60×60	3.55E-06	3.59	1.36E-06	6.67	5.39E-07	3.03	8.57E-07	4.11
	80×80	2.94E-06	0.65	6.78E-06	-5.58	2.28E-07	2.99	1.01E-06	-0.58

Since we do not know the explicit exact solutions to this problem, we adopt the a posterior errors $\|u_h - u_{\frac{h}{2}}\|$ as the numerical errors to compute the convergence rate. We first use the uniform tensor product meshes Ω_h with nodes (x_i, y_j), where $\{x_i\}_{i=0}^{2N}$, $\{y_j\}_{j=0}^{2N}$ such that $x_i = \frac{\pi}{N} i, y_j = \frac{\pi}{N} j$ for $i, j = 0, 1, \ldots, 2N$. The results are listed in Table 4.9, from which we can see that the UWLDG scheme is stable but the optimal convergence rate cannot be observed due to the corner singularity.

To recover the loss of accuracy, we consider a special tensor product mesh in the way that the initial mesh in x and y direction are given as a geometric proportional mesh approaching to the corner, and then refine the mesh by dividing each cell into two equal-sized subcells. To be more specific, taking the x direction as an example, the i-th cell length, denoted by h_i^x, is defined as

$$h_1^x = h_{2N_0}^x = \frac{\pi(1-\sigma)}{1-\sigma^{N_0}},$$
$$h_i^x = h_{2N_0+1-i}^x = \sigma h_{i-1}^x, \ i = 2, \ldots, N_0,$$

where $2N_0$ denotes the total number of cells in x direction, and $\sigma < 1$ is the common ratio. Then $\{x_i\}_{i=0}^{2N_0}$ is determined by $x_i = x_{i-1} + h_i^x$ with $x_0 = 0$, and the tensor product initial mesh in the L-shape domain is obtained by taking $y_i = x_i$, as shown in Figure 4.3(a) with $\sigma = 0.4, N_0 = 4$, and the corresponding refined mesh is shown in Figure 4.3(b).

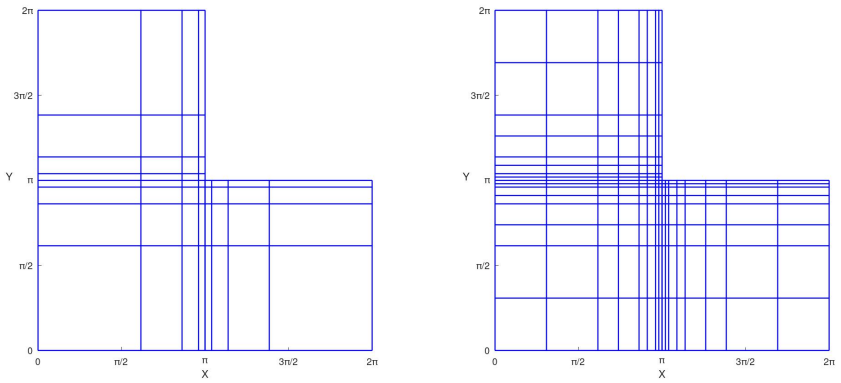

(a) The initial mesh for $N_0 = 4$.

(b) The refined mesh for $N = 8$.

FIGURE 4.3. The initial mesh for $N_0 = 4$ with $\sigma = 0.4$ and the refined mesh for $N = 8$.

We use $\mathcal{Q}^1$ and $\mathcal{Q}^2$ polynomials to test the numerical solution on the refined mesh with $\sigma = 0.6$ and $\sigma = 0.4$, respectively. L^2 errors and orders of $\|u_h - u_{\frac{h}{2}}\|$ are also given in Table 4.9. We can see that, both for $\mathcal{Q}^1$ and $\mathcal{Q}^2$ polynomials, the order of accuracy is improved to about $k+1$, and a smaller amplitude of the errors is observed when compared with uniform meshes.

TABLE 4.9. L^2 errors $\|u_h - u_{\frac{h}{2}}\|$ and orders for the singular problem (4.1a)–(4.1c) in an L-shape domain with a uniform and refined mesh.

	N	uniform mesh		refined mesh	
		$\|u_h - u_{\frac{h}{2}}\|$	order	$\|u_h - u_{\frac{h}{2}}\|$	order
$\mathcal{Q}^1$	4	2.81E-01	–	1.30E-01	–
	8	1.65E-02	–	1.28E-01	–
	16	1.22E-03	3.75	7.21E-03	4.15
	32	3.86E-04	1.66	2.89E-04	4.63
	64	2.00E-04	0.95	5.14E-05	2.49
$\mathcal{Q}^2$	4	3.03E-02	–	3.42E-02	–
	8	1.10E-03	–	3.34E-02	–
	16	3.90E-04	1.49	3.26E-04	7.06
	32	1.67E-04	1.22	3.78E-05	3.10

5. Concluding remarks

In this paper, we analyze the UWLDG method solving time-dependent linear fourth-order equations with four types of boundary conditions. By designing elaborate numerical fluxes together with some penalty terms and constructing suitable projections, stability and optimal error estimates are derived, which are valid for one- and two-dimensional problems. Numerical experiments are presented to illustrate the sharpness of theoretical results. The treatment of various boundary conditions of this work would be helpful for solving other practical engineering problems involving complex boundary conditions. Inspired by [7], extension of this work to simplicial meshes and other high order equations constitutes our future work.

Appendix A. Proof of a few technical lemmas

A.1. The proof of Lemma 3.11.

Proof. • **The proof for** (3.27a) **:** $\boldsymbol{K \in \Omega_h^I}$.

By (3.9), we have the following specific expression of $B_K(\eta_w, p)$

$$B_K(\eta_w, p) = \sum_{m=0}^{8} T_m^{ij}(\eta_w, p), \quad K = K_{ij} \in \Omega_h^I, \tag{A.1}$$

where $T_m^{ij}(\eta_w, p)$ are defined by (3.10). Since Π is a polynomial preserving operator up to k, then (3.27a) holds for each $w \in \mathcal{Q}^k(K)$. Thus, we only need to consider the cases

$$w(x,y) = x^{k+2},\ y^{k+2},\ x^{k+1}y,\ y^{k+1}x,\ x^{k+1},\ y^{k+1}. \tag{A.2}$$

For $w(x,y) = x^{k+2}$, since it only depends on x, we have $\Pi w = \mathsf{P}_{M_x}(x^{k+2})$. Clearly, $(\eta_w)_y = 0$. Then, by the definition of P_M, we have

$$T_m^{ij}(\eta_w, p) = 0, \quad m = 1,2,5,6,7,8, \quad \int_{K_{ij}} (w - \Pi w)\, p_{xx} dxdy = 0.$$

In addition, we use integration by parts to find that

$$\int_{K_{ij}} (w - \Pi w)\, p_{yy} dxdy = -\, T_3^{ij}(\eta_w, p) - T_4^{ij}(\eta_w, p).$$

A substitution of above results into (A.1) leads to

$$B_K(\eta_w, p) = 0, \text{ if } w(x,y) = x^{k+2}.$$

For $w(x,y) = yx^{k+1}$, we have $\Pi w = y\mathsf{P}_{M_x}(x^{k+1})$, hence

$$T_m^{ij}(\eta_w, p) = 0,\ m = 1,2,5,6, \quad \int_{K_{ij}} (w - \Pi w)\, p_{xx} dxdy = 0.$$

Besides, we use integration by parts twice to find that

$$\int_{K_{ij}} (w - \Pi w)\, p_{yy} dxdy = -\, T_3^{ij}(\eta_w, p) - T_4^{ij}(\eta_w, p) - T_7^{ij}(\eta_w, p) - T_8^{ij}(\eta_w, p).$$

Substituting above results into (A.1), we get

$$B_K(\eta_w, p) = 0, \text{ if } w(x,y) = yx^{k+1}.$$

For $w(x,y) = y^{k+2},\ y^{k+1}x,\ x^{k+1}$ and y^{k+1}, the proofs are analogous, and thus omitted. This finishes the proof of (3.27a).

• **The proof for** (3.27b) **:** $\boldsymbol{K \in \Omega_h^0}$.
We take $K = K_{11}$ as an example. By (3.23c)–(3.23d), we have

$$B_{K_{11}}(\eta_w, p) = \sum_{m=0}^{5} T_m^{11}(\eta_w, p) + \big(\widetilde{T}_6^{11} + T_7^{11} + \widetilde{T}_8^{11}\big)(\eta_w, p), \tag{A.3}$$

where $T_m^{11}(\eta_w, p),\ m = 0, 1, 2, 3, 4, 5, 7$ are determined by (3.10) for $i, j = 1$, and

$$\widetilde{T}_6^{11}(\eta_w, p) = -\int_{J_1} (\eta_w)_x\big(x_{\frac{1}{2}}^+, y\big)\, p\big(x_{\frac{1}{2}}^+, y\big)\, dy,\ \widetilde{T}_8^{11}(\eta_w, p) = -\int_{I_1} (\eta_w)_y\big(x, y_{\frac{1}{2}}^+\big)\, p\big(x, y_{\frac{1}{2}}^+\big) dx.$$

We still only need to consider the cases in (A.2). First, for $w(x, y) = x^{k+2}$, we have $\Pi w = \mathsf{P}_{M_x}(x^{k+2})$, $(\eta_w)_y = 0$. Therefore,

$$T_m^{11}(\eta_w, p) = 0,\ m = 1, 2, 5, 7, \quad \widetilde{T}_8^{11}(\eta_w, p) = 0, \quad \int_{K_{11}} (w - \Pi w)\, p_{xx} dx dy = 0.$$

We use integration by parts to find that

$$\int_{K_{11}} (w - \Pi w) p_{yy}\, dx dy = -T_3^{11}(\eta_w, p) - T_4^{11}(\eta_w, p).$$

Substitute above results into (A.3) to get

$$B_{K_{11}}(\eta_w, p) = \widetilde{T}_6^{11}(\eta_w, p), \quad \text{if } w(x, y) = x^{k+2}.$$

Next, we consider $w(x, y) = xy^{k+1}$. Clearly, $\Pi w = x\mathsf{P}_{M_y}(y^{k+1})$. By the definition of P_M, we immediately have

$$T_m^{11}(\eta_w, p) = 0,\ m = 3, 4, 7, \quad \int_{K_{11}} (w - \Pi w) p_{yy}\, dx dy = 0.$$

Furthermore, using integration by parts twice, we arrive at

$$\int_{K_{11}} (w - \Pi w) p_{xx}\, dx dy = -\big(T_1^{11} + T_2^{11} + T_5^{11} + \widetilde{T}_6^{11}\big)(\eta_w, p).$$

A substitution of above results into (A.3) gives us

$$B_{K_{11}}(\eta_w, p) = \widetilde{T}_8^{11}(\eta_w, p), \quad \text{if } w(x, y) = xy^{k+1}. \tag{A.4}$$

Similarly, it is easy to check that

$$\begin{aligned} B_{K_{11}}(\eta_w, p) &= \widetilde{T}_6^{11}(\eta_w, p), \quad \text{if } w(x, y) = x^{k+1},\ yx^{k+1}, \\ B_{K_{11}}(\eta_w, p) &= \widetilde{T}_8^{11}(\eta_w, p), \quad \text{if } w(x, y) = y^{k+1},\ y^{k+2}. \end{aligned}$$

Finally, we conclude that for all $w \in \mathcal{P}^{k+2}$, there are at most two nonzero terms $\widetilde{T}_6^{11}(\eta_w, p)$ and $\widetilde{T}_8^{11}(\eta_w, p)$ in $B_{K_{11}}(\eta_w, p)$, i.e.,

$$B_{K_{11}}(\eta_w, p) = -\int_{J_1} (\eta_w)_x\big(x_{\frac{1}{2}}^+, y\big) p\big(x_{\frac{1}{2}}^+, y\big)\, dy - \int_{I_1} (\eta_w)_y\big(x, y_{\frac{1}{2}}^+\big) p\big(x, y_{\frac{1}{2}}^+\big)\, dx.$$

For other boundary elements, we can use a similar analysis as above for the case of K_{11}. Therefore, to derive (3.27b), we need only to sum over the results derived by all K in Ω_h^0, and this completes the proof of (3.27b). □

A.2. **The proof of Lemma 3.12.**

Proof. • $\boldsymbol{K \in \Omega_h^I}$.

For interelements $K \in \Omega_h^I$, using the same analysis as that in the proof of (3.27a), we can easily obtain

$$B_K(\eta_u, q) = 0, \quad \forall u \in \mathcal{P}^{k+2},\ K \in \Omega_h^I.$$

• $\boldsymbol{K \in \Omega_h^0}$.

For the boundary elements $K \in \Omega_h^0$, without loss of generality, consider $K = K_{11}$ as an example. By (3.23a) and (3.23b), we get

$$B_{K_{11}}(\eta_u, q) = (T_0^{11} + T_1^{11} + T_3^{11} + T_5^{11} + T_7^{11})(\eta_u, q) + \sum_{m=1}^{4} S_m^{11}(u, q), \tag{A.5}$$

where $T_m^{11}(\eta_u, q),\ m = 0, 1, 3, 5, 7$ are determined by (3.10) for $i,\ j = 1$, and

$$\begin{aligned}
S_1^{11}(u,q) &= -\int_{I_1} \Big(u_y\big(x, y_{\frac{1}{2}}\big) - \mathsf{P}_{M_x}\big(u_y(x, y_{\frac{1}{2}})\big)\Big)\, q\big(x, y_{\frac{1}{2}}^+\big)\, dx,\\
S_2^{11}(u,q) &= \int_{I_1} \Big(u\big(x, y_{\frac{1}{2}}\big) - \mathsf{P}_{M_x}\big(u(x, y_{\frac{1}{2}})\big)\Big)\, q_y\big(x, y_{\frac{1}{2}}^+\big)\, dx,\\
S_3^{11}(u,q) &= -\int_{J_1} \Big(u_x\big(x_{\frac{1}{2}}, y\big) - \mathsf{P}_{M_y}\big(u_x(x_{\frac{1}{2}}, y)\big)\Big)\, q\big(x_{\frac{1}{2}}^+, y\big)\, dy,\\
S_4^{11}(u,q) &= \int_{J_1} \Big(u\big(x_{\frac{1}{2}}, y\big) - \mathsf{P}_{M_y}\big(u(x_{\frac{1}{2}}, y)\big)\Big)\, q_x\big(x_{\frac{1}{2}}^+, y\big)\, dy.
\end{aligned}$$

We still only need to check the cases in (A.2), since P_M and Π are all polynomial preserving operators up to k.

For $u(x, y) = x^{k+2}$, we have $\Pi u = \mathsf{P}_{M_x}(x^{k+2})$, then $u_y = (\Pi u)_y = 0$. Hence, combining with the properties of the P_M, we have

$$T_1^{11}(\eta_u, q) = T_5^{11}(\eta_u, q) = T_7^{11}(\eta_u, q) = S_1^{11}(u, q) = 0, \quad \int_{K_{11}} (u - \Pi u)\, q_{xx} dxdy = 0.$$

Furthermore, using integration by parts, we can find that,

$$\int_{K_{11}} (u - \Pi u)\, q_{yy} dxdy = -T_3^{11}(\eta_u, q) - S_2^{11}(u, q).$$

In addition, since P_M is polynomial preserving for $k \geq 1$, then

$$\begin{aligned}
S_3^{11}(u,q) &= -\int_{J_1} \Big((k+2)\big(x_{\frac{1}{2}}\big)^{k+1} - \mathsf{P}_{M_y}\big((k+2)\big(x_{\frac{1}{2}}\big)^{k+1}\big)\Big)\, q\big(x_{\frac{1}{2}}^+, y\big)\, dy = 0,\\
S_4^{11}(u,q) &= \int_{J_1} \Big(\big(x_{\frac{1}{2}}\big)^{k+2} - \mathsf{P}_{M_y}\big((x_{\frac{1}{2}})^{k+2}\big)\Big)\, q_x\big(x_{\frac{1}{2}}^+, y\big)\, dy = 0.
\end{aligned}$$

Collecting above results into (A.5), we obtain

$$B_{K_{11}}(\eta_u, q) = 0, \quad \text{if } u = x^{k+2}.$$

For $u(x, y) = yx^{k+1}$, $\Pi u = y\mathsf{P}_{M_x}(x^{k+1})$. Then

$$T_1^{11}(\eta_u, q) = 0, \quad T_5^{11}(\eta_u, q) = 0, \ \int_{K_{11}} (u - \Pi u)\, q_{xx} dxdy = 0.$$

Again, the fact P_M is polynomial preserving for $k \geq 1$ leads to

$$S_3^{11}(u,q) = -\int_{J_1} \Big((k+1)\big(x_{\frac{1}{2}}\big)^k y - \mathsf{P}_{M_y}\big((k+1)\big(x_{\frac{1}{2}}\big)^k y\big)\Big)\, q\big(x_{\frac{1}{2}}^+, y\big)\, dy = 0,$$

$$S_4^{11}(u,q) = \int_{J_1} \Big(\big(x_{\frac{1}{2}}\big)^{k+1} y - \mathsf{P}_{M_y}\big((x_{\frac{1}{2}})^{k+1} y\big)\Big)\, q_x\big(x_{\frac{1}{2}}^+, y\big)\, dy = 0.$$

Using integration by parts twice, we can find that

$$\int_{K_{11}} (u - \Pi u)\, q_{yy} dx dy = -T_3^{11}(\eta_u, q) - T_7^{11}(\eta_u, q) - S_1^{11}(u,q) - S_2^{11}(u,q).$$

Substituting above results into (A.5), we arrive at

$$B_{K_{11}}(\eta_u, q) = 0, \quad \text{if } u(x,y) = yx^{k+1}.$$

For other cases $u(x,y) = y^{k+2}, xy^{k+1}, x^{k+1}, y^{k+1}$, the proofs are analogous. Therefore, we have $B_{K_{11}}(\eta_u, q) = 0,\ \forall u \in \mathcal{P}^{k+2}$. Analysis for other boundary elements K_{ij} can be performed similarly. This completes the proof of (3.28). □

A.3. **The proof of Lemma 3.13.**

Proof. • $\boldsymbol{K \in \Omega_h^I}$.

Since $k \geq 1$, by the Cauchy–Schwarz inequality, the approximation property of the projection Π, trace and inverse inequalities, we can establish the following rough estimate: for any $v \in H^2(\Omega_h)$ and $K \in \Omega_h^I$,

$$\begin{aligned} \big|B_K(\eta_v, p)\big| &\leq \|\eta_v\|_K \|\Delta p\|_K + C\|\eta_v\|_{\partial\widetilde{K}} \|\nabla p\|_{\partial K} + C\|\nabla \eta_v\|_{\partial\widetilde{K}} \|p\|_{\partial K} \\ &\leq Ch^2 \|v\|_{2,K} h^{-2} \|p\|_K + Ch^{\frac{3}{2}} \|v\|_{2,\widetilde{K}} h^{-\frac{3}{2}} \|p\|_K + Ch^{\frac{1}{2}} \|v\|_{2,\widetilde{K}} h^{-\frac{1}{2}} \|p\|_K \\ &\leq C\|v\|_{2,\widetilde{K}} \|p\|_K, \end{aligned} \tag{A.6}$$

where $\widetilde{K} = \{K_{i+1,j},\ K_{i-1,j},\ K_{ij},\ K_{i,j-1},\ K_{i,j+1}\}$. Let χ be any polynomial of degree at most $k+2$, by (3.27a) in Lemma 3.11, we have

$$B_K(\eta_\chi, p) = 0,\ \forall p \in W_h.$$

Then, by the linearity of operator $B_K(\cdot, p)$ and the estimate (A.6), we get

$$B_K(\eta_w, p) = B_K(\eta_w, p) - B_K(\eta_\chi, p) = B_K(\eta_{w-\chi}, p) \leq C\|w - \chi\|_{2,\widetilde{K}} \|p\|_K.$$

Consequently, for all $K \in \Omega_h^I$

$$\big|B_K(\eta_w, p)\big| \leq C \inf_{\chi \in \mathcal{P}^{k+2}} \|w - \chi\|_{2,\widetilde{K}} \|p\|_K \leq Ch^{k+1} \|w\|_{k+3,\widetilde{K}} \|p\|_K, \tag{A.7}$$

which produces

$$\sum_{K \in \Omega_h^I} |B_K(\eta_w, p)| \leq Ch^{k+1} \|w\|_{k+3} \|p\|. \tag{A.8}$$

• $\boldsymbol{K \in \Omega_h^0}$.

We take the element $K = K_{11}$ as an example. Recalling (A.3), we split $B_{K_{11}}(\eta_w, p)$ into two parts

$$B_{K_{11}}(\eta_w, p) = A_{K_{11}}(\eta_w, p) + \widetilde{A}_{K_{11}}(\eta_w, p),$$

where

$$A_{K_{11}}(\eta_w, p) = \sum_{m=0}^{5} T_m^{11}(\eta_w, p) + T_7^{11}(\eta_w, p),\ \ \widetilde{A}_{K_{11}}(\eta_w, p) = \widetilde{T}_6^{11}(\eta_w, p) + \widetilde{T}_8^{11}(\eta_w, p).$$

Notice that we have checked that $A_{K_{11}}(\eta_\chi, p) = 0$ holds for any $\chi \in \mathcal{P}^{k+2}(K_{11})$ in the proof of (3.27b), then $A_{K_{11}}(\eta_w, p)$ can be estimated by using the same skill as that for interelements in (A.7). It reads,

$$|A_{K_{11}}(\eta_w, p)| \le Ch^{k+1}\|w\|_{k+3,\widetilde{K_{11}}}\|p\|_{K_{11}}, \tag{A.9}$$

where $\widetilde{K_{11}} = \{K_{21},\ K_{11},\ K_{12}\}$. By Young's inequality, we have

$$\begin{aligned}|\widetilde{A}_{K_{11}}(\eta_w, p)| \le \frac{h^3}{2k_3}\int_{J_1}|(\eta_w)_x(x^+_{\frac{1}{2}}, y)|^2dy + \frac{k_3}{2h^3}\int_{J_1}|p(x^+_{\frac{1}{2}}, y)|^2dy \\ + \frac{h^3}{2k_4}\int_{I_1}|(\eta_w)_y(x, y^+_{\frac{1}{2}})|^2dx + \frac{k_4}{2h^3}\int_{I_1}|p(x, y^+_{\frac{1}{2}})|^2dx.\end{aligned}$$

Furthermore, using the trace inequality and the approximation properties of Π, we obtain

$$\begin{aligned}\int_{J_1}|(\eta_w)_x(x^+_{\frac{1}{2}}, y)|^2dy \le \|(\eta_w)_x\|^2_{\partial K_{11}} \le Ch^{2k-1}\|w\|^2_{k+1,K_{11}}, \\ \int_{I_1}|(\eta_w)_y(x, y^+_{\frac{1}{2}})|^2dx \le \|(\eta_w)_y\|^2_{\partial K_{11}} \le Ch^{2k-1}\|w\|^2_{k+1,K_{11}}.\end{aligned}$$

Therefore, we arrive at the estimate of $\widetilde{A}_{K_{11}}(\eta_w, p)$ as

$$|\widetilde{A}_{K_{11}}(\eta_w, p)| \le Ch^{2k+2}\|w\|^2_{k+1,K_{11}} + \frac{k_3}{2h^3}\int_{J_1}|p(x^+_{\frac{1}{2}}, y)|^2dy + \frac{k_4}{2h^3}\int_{I_1}|p(x, y^+_{\frac{1}{2}})|^2dx.$$

Combining the above estimate with (A.9), we get

$$\begin{aligned}|B_{K_{11}}(\eta_w, p)| \le Ch^{k+1}\|w\|_{k+3,\widetilde{K_{11}}}\|p\|_{K_{11}} + Ch^{2k+2}\|w\|^2_{k+1,K_{11}} \\ + \frac{k_3}{2h^3}\int_{J_1}|p(x^+_{\frac{1}{2}}, y)|^2dy + \frac{k_4}{2h^3}\int_{I_1}|p(x, y^+_{\frac{1}{2}})|^2dx.\end{aligned} \tag{A.10}$$

For the cases of other boundary elements, similar estimates as (A.10) can also be derived. Summing over all elements in Ω^0_h, we deduce that

$$\begin{aligned}\sum_{K\in\Omega^0_h}|B_K(\eta_w, p)| &\le Ch^{k+1}\sum_{K\in\Omega^0_h}\|w\|_{k+3,\widetilde{K}}\|p\|_K + Ch^{2k+2}\sum_{K\in\Omega^0_h}\|w\|^2_{k+1,K} + \frac{1}{2}S(p), \\ &\le Ch^{k+1}\|w\|_{k+3}\|p\| + Ch^{2k+2}\|w\|^2_{k+1} + \frac{1}{2}S(p),\end{aligned} \tag{A.11}$$

where $\widetilde{K} \subseteq \Omega_h$ denotes the union of K and all of its neighbor elements in Ω_h. The expected estimate (3.29) follows by combining (A.8) and (A.11). □

A.4. **The proof of Lemma 3.14.**

Proof. • $\boldsymbol{K \in \Omega^I_h}$.

By Lemma 3.12, we know

$$B_K(\eta_\chi, q) = 0,\ \forall\chi \in \mathcal{P}^{k+2}(K),\ q \in W_h.$$

And we also have the rough estimate as in (A.6), it reads

$$|B_K(\eta_v, q)| \le C\|v\|_{2,\widetilde{K}}\|q\|_K, \quad \forall v \in H^2(\Omega_h),\ K \in \Omega_h,\ q \in W_h.$$

Hence, using the same argument as that in the proof of (A.7), we arrive at

$$|B_K(\eta_u, q)| \le Ch^{k+1}\|u\|_{k+3,\widetilde{K}}\|q\|_K,\ \forall K \in \Omega^I_h. \tag{A.12}$$

- $\boldsymbol{K \in \Omega_h^0}$.

We still take K_{11} as an example and recall the expression of $B_{K_{11}}(\eta_u, q)$ in (A.5),

$$B_{K_{11}}\big(\eta_u, q\big) = (T_0^{11} + T_1^{11} + T_3^{11} + T_5^{11} + T_7^{11})(\eta_u, q) + \sum_{m=1}^{4} S_m^{11}(u, q).$$

Similar to the proof of (A.6), it is easy to get

$$\big|(T_0^{11} + T_1^{11} + T_3^{11} + T_5^{11} + T_7^{11})(\eta_u, q)\big| \le C\|u\|_{2,\widetilde{K_{11}}}\|q\|_{K_{11}}.$$

In addition, by the Cauchy-Schwarz inequality, approximation property of the one-dimensional projection P_M, trace and inverse inequalities, we obtain

$$\begin{aligned}
\big|S_1^{11}(u,q) + S_3^{11}(u,q)\big| &\le \|u_y(\cdot, y_{\frac12}) - \mathsf{P}_{M_x}\big(u_y(\cdot, y_{\frac12})\big)\|_{I_1}\|q(\cdot, y_{\frac12}^+)\|_{I_1} \\
&\quad + \|u_x(x_{\frac12}, \cdot) - \mathsf{P}_{M_y}\big(u_x(x_{\frac12}, \cdot)\big)\|_{J_1}\|q(x_{\frac12}^+, \cdot)\|_{J_1} \\
&\le Ch^2\big(\,\|u_y(\cdot, y_{\frac12})\|_{2,I_1} + \|u_x(x_{\frac12}, \cdot)\|_{2,J_1}\,\big)\|q\|_{\partial K_{11}} \\
&\le Ch^{\frac32}\|u\|_{4,K_{11}}\|q\|_{K_{11}},
\end{aligned}$$

and

$$\begin{aligned}
\big|S_2^{11}(u,q) + S_4^{11}(u,q)\big| &\le \|\eta_u(\cdot, y_{\frac12}^+)\|_{I_1}\|q_y(\cdot, y_{\frac12}^+)\|_{I_1} + \|\eta_u(x_{\frac12}^+, \cdot)\|_{J_1}\|q_x(x_{\frac12}^+, \cdot)\|_{J_1} \\
&\le \|\eta_u\|_{\partial K_{11}} \cdot \big(\|q_y\|_{\partial K_{11}} + \|q_x\|_{\partial K_{11}}\big) \\
&\le C\|u\|_{2,K_{11}}\|q\|_{K_{11}}.
\end{aligned}$$

Thus, we arrive at the rough estimate for $B_{K_{11}}\big(\eta_u, q\big)$ as

$$|B_{K_{11}}\big(\eta_u, q\big)| \le C\|u\|_{4,\widetilde{K_{11}}}\|q\|_{K_{11}}.$$

From Lemma 3.12, we also know

$$B_{K_{11}}\left(\eta_\chi, q\right) = 0,\ \forall \chi \in \mathcal{P}^{k+2}(K_{11}),\ q \in W_h,$$

then using a similar argument as that in the proof of (A.7) again, we can obtain

$$|B_{K_{11}}\big(\eta_u, q\big)| \le Ch^{k+1}\|u\|_{k+5,\widetilde{K_{11}}}\|q\|_{K_{11}}.$$

Analogously, we can check that, for any other boundary elements $K_{ij} \in \Omega_h^0$, the above estimate holds, i.e.,

$$|B_{K_{ij}}\big(\eta_u, q\big)| \le Ch^{k+1}\|u\|_{k+5,\widetilde{K_{ij}}}\|q\|_{K_{ij}}, \quad \forall K_{ij} \in \Omega_h^0, \tag{A.13}$$

where $\widetilde{K_{ij}} \subseteq \Omega_h$ denotes the union of K_{ij} and all of its neighbor elements in Ω_h. Therefore, the estimate (3.30) follows by combining (A.12)–(A.13) and summing over all $K \in \Omega_h$. □

References

1. G. A. Baker, *Finite element methods for elliptic equations using nonconforming elements*, Math. Comp. **31** (1977), no. 137, 45–59, DOI 10.2307/2005779. MR 431742
2. H. Blum and R. Rannacher, R.and Leis, *On the boundary value problem of the biharmonic operator on domains with angular corners*, Math. Methods Appl. Sci. **2** (1980), no. 4, 556–581, DOI 10.1002/mma.1670020416. MR 595625
3. S. C. Brenner, S. Gu, T. Gudi, and L.-Y. Sung, *A quadratic C° interior penalty method for linear fourth order boundary value problems with boundary conditions of the Cahn–Hilliard type*, SIAM J. Numer. Anal. **50** (2012), no. 4, 2088–2110, DOI 10.1137/110847469. MR 3022211

4. I. C. Dolcetta, S. F. Vita, and R. March, *Area-preserving curve-shortening flows: from phase separation to image processing*, Interfaces Free Bound. **4** (2002), no. 4, 325–343, DOI 10.4171/ifb/64. MR 1935642
5. J. W. Cahn and J. E. Hilliard, *Free energy of a nonuniform system. I. Interfacial free energy*, J. Chem. Phys. **28** (1958), no. 2, 258–267, DOI 10.1063/1.1744102.
6. P. Castillo, B. Cockburn, D. Schötzau, and C. Schwab, *Optimal a priori error estimates for the hp-version of the local discontinuous Galerkin method for convection-diffusion problems*, Math. Comp. **71** (2002), no. 238, 455–478, DOI 10.1090/S0025-5718-01-01317-5. MR 1885610
7. Y. Chen and Y. Xing, *Optimal error estimates of ultra-weak discontinuous Galerkin methods with generalized numerical fluxes for multi-dimensional convection-diffusion and biharmonic equations*, Math. Comp. (2023), DOI 10.1090/mcom/3927.
8. Y. Cheng and C.-W. Shu, *A discontinuous Galerkin finite element method for time dependent partial differential equations with higher order derivatives*, Math. Comp. **77** (2007), no. 262, 699–730, DOI 10.1090/s0025-5718-07-02045-5. MR 2373176
9. P. G. Ciarlet, *The finite element method for elliptic problems*, Classics in Applied Mathematics, vol. 40, Society for Industrial and Applied Mathematics (SIAM), Philadelphia, PA, 2002, Reprint of the 1978 original [North-Holland, Amsterdam; MR0520174 (58 #25001)]. MR 1930132
10. B. Cockburn and B. Dong, *An analysis of the minimal dissipation local discontinuous Galerkin method for convection-diffusion problems*, J. Sci. Comput. **32** (2007), no. 2, 233–262, DOI 10.1007/s10915-007-9130-3. MR 2320571
11. B. Cockburn, B. Dong, and J. Guzmán, *A hybridizable and superconvergent discontinuous Galerkin method for biharmonic problems*, J. Sci. Comput. **40** (2009), no. 1-3, 141–187, DOI 10.1007/s10915-009-9279-z. MR 2511731
12. B. Cockburn and C.-W. Shu, *The local discontinuous Galerkin method for time-dependent convection-diffusion systems*, SIAM J. Numer. Anal. **35** (1998), no. 6, 2440–2463, DOI 10.1137/s0036142997316712. MR 1655854
13. V. Dolejší and M. Feistauer, *Discontinuous Galerkin method. Analysis and applications to compressible flow*, Springer Ser. Comput. Math., vol. 48, Springer, Cham, 2015, DOI 10.1007/978-3-319-19267-3. MR 3363720
14. B. Dong and C.-W. Shu, *Analysis of a local discontinuous Galerkin method for linear time-dependent fourth-order problems*, SIAM J. Numer. Anal. **47** (2009), no. 5, 3240–3268, DOI 10.1137/080737472. MR 2551193
15. Z. Dong, L. Mascotto, and O. J. Sutton, *Residual-based a posteriori error estimates for hp-discontinuous Galerkin discretizations of the biharmonic problem*, SIAM J. Numer. Anal. **59** (2021), no. 3, 1273–1298, DOI 10.1137/20M1364114. MR 4257874
16. G. Engel, K. Garikipati, T. J. R. Hughes, M. G. Larson, L. Mazzei, and R. L. Taylor, *Continuous/discontinuous finite element approximations of fourth-order elliptic problems in structural and continuum mechanics with applications to thin beams and plates, and strain gradient elasticity*, Comput. Methods Appl. Mech. Engrg. **191** (2002), no. 34, 3669–3750, DOI 10.1016/s0045-7825(02)00286-4. MR 1915664
17. X. Feng and O. A. Karakashian, *Fully discrete dynamic mesh discontinuous Galerkin methods for the Cahn-Hilliard equation of phase transition*, Math. Comp. **76** (2007), no. 259, 1093–1117, DOI 10.1090/S0025-5718-07-01985-0. MR 2299767
18. E. H. Georgoulis and P. Houston, *Discontinuous Galerkin methods for the biharmonic problem*, IMA J. Numer. Anal. **29** (2009), no. 3, 573–594, DOI 10.1093/imanum/drn015. MR 2520159
19. T. Gudi, N. Nataraj, and A. K. Pani, *Mixed discontinuous Galerkin finite element method for the biharmonic equation*, J. Sci. Comput. **37** (2008), no. 2, 139–161, DOI 10.1007/s10915-008-9200-1. MR 2453216
20. J. Li, D. Zhang, X. Meng, and B. Wu, *Analysis of local discontinuous Galerkin methods with generalized numerical fluxes for linearized KdV equations*, Math. Comp. **89** (2020), no. 325, 2085–2111, DOI 10.1090/mcom/3550. MR 4109561
21. H. Liu and P. Yin, *A mixed discontinuous Galerkin method without interior penalty for time-dependent fourth order problems*, J. Sci. Comput. **77** (2018), no. 1, 467–501, DOI 10.1007/s10915-018-0756-0. MR 3850361

22. Y. Liu, Q. Tao, and C.-W. Shu, *Analysis of optimal superconvergence of an ultraweak-local discontinuous Galerkin method for a time dependent fourth-order equation*, ESAIM Math. Model. Numer. **54** (2020), no. 6, 1797–1820, DOI 10.1051/m2an/2020023. MR 4129382
23. E. Y. Medina, E. M. Toledo, I. Igreja, and B. M. Rocha, *A stabilized hybrid discontinuous Galerkin method for the Cahn-Hilliard equation*, J. Comput. Appl. Math. **406** (2022), Paper No. 114025, DOI 10.1016/j.cam.2021.114025. MR 4360352
24. X. Meng, C.-W. Shu, and B. Wu, *Superconvergence of the local discontinuous Galerkin method for linear fourth-order time-dependent problems in one space dimension*, IMA J. Numer. Anal. **32** (2012), no. 4, 1294–1328, DOI 10.1093/imanum/drr047. MR 2991829
25. I. Mozolevski and E. Süli, *A priori error analysis for the hp-version of the discontinuous Galerkin finite element method for the biharmonic equation*, Comput. Methods Appl. Math. **3** (2003), no. 4, 596–607, DOI 10.2478/cmam-2003-0037. MR 2048235
26. C.-W. Shu, *Discontinuous Galerkin method for time-dependent problems: survey and recent developments*, IMA Vol. Math. Appl., vol. 157, Springer, Cham, 2014, DOI 10.1007/978-3-319-01818-8_2. MR 3203111
27. E. Süli and I. Mozolevski, *hp-version interior penalty DGFEMs for the biharmonic equation*, Comput. Methods Appl. Mech. Engrg. **196** (2007), no. 13-16, 1851–1863, DOI 10.1016/j.cma.2006.06.014. MR 2298696
28. Q. Tao, W. Cao, and Z. Zhang, *Superconvergence analysis of the ultra-weak local discontinuous Galerkin method for one dimensional linear fifth order equations*, J. Sci. Comput. **88** (2021), no. 3, Paper No. 63, DOI 10.1007/s10915-021-01579-9. MR 4291691
29. Q. Tao, Y. Xu, and C.-W. Shu, *An ultraweak-local discontinuous Galerkin method for PDEs with high order spatial derivatives*, Math. Comp. **89** (2020), no. 326, 2753–2783, DOI 10.1090/mcom/3562. MR 4136546
30. ———, *A discontinuous Galerkin method and its error estimate for nonlinear fourth-order wave equations*, J. Comput. Appl. Math. **386** (2021), Paper No. 113230, DOI 10.1016/j.cam.2020.113230. MR 4167183
31. G. N. Wells, E. Kuhl, and K. Garikipati, *A discontinuous Galerkin method for the Cahn–Hilliard equation*, J. Comput. Phys. **218** (2006), no. 2, 860–877, DOI 10.1016/j.jcp.2006.03.010. MR 2269388
32. Y. Xu and C.-W. Shu, *Optimal error estimates of the semidiscrete local discontinuous Galerkin methods for high order wave equations*, SIAM J. Numer. Anal. **50** (2012), no. 1, 79–104, DOI 10.1137/11082258x. MR 2888305

School of Mathematics, Harbin Institute of Technology, Harbin 150001, Heilongjiang, People's Republic of China
E-mail address: fengyu_fu@stu.hit.edu.cn

Division of Applied Mathematics, Brown University, Providence, RI 02912
E-mail address: chi-wang_shu@brown.edu

School of Mathematics, Statistics and Mechanics, Beijing University of Technology, Beijing 100124, People's Republic of China
E-mail address: taoqi@bjut.edu.cn

School of Mathematics, Harbin Institute of Technology, Harbin 150001, Heilongjiang, People's Republic of China
E-mail address: mathwby@hit.edu.cn